Smart Materials, Chemical Systems, and Digital Technologies

Dr. R. MURALIRAJA
Mrs. DIMPLE JUNEJA
Dr. A. R. SIVARAM
Dr. S. GNANAM

SRR
Publicizing Research

ISBN 978-816855382-8

Smart Materials, Chemical Systems, and Digital Technologies

April 2026

Dr. R. MURALIRAJA
Associate Professor, Department of Mechanical Engineering
Vels Institute of Science, Technology & Advanced Studies (VISTAS), Chennai, Tamil Nadu, India.

Mrs. DIMPLE JUNEJA
Research Scholar, Department of Education
Mohanlal Sukhadia University
Udaipur, Rajasthan, India.

Dr. A. R. SIVARAM
Assistant Professor
Department of Naval Architecture and Offshore Engineering
Academy of Maritime Education and Training (AMET)
Chennai, Tamil Nadu, India.

Dr. S. GNANAM
Assistant Professor
Department of Physics, School of Basic Sciences
Vels Institute of Science, Technology & Advanced Studies (VISTAS), Chennai, Tamil Nadu, India.

April 2026

ISBN: 978-81-685538-2-8

Published By

SRR
Publicizing Research

SCIENTIFIC RESEARCH REPORTS
(A Book Publisher, approved by Govt. of India)

I Floor, S S Nagar, Chennai - 600 087,
Tamil Nadu, India.

editors@srrbooks.in, contact@srrbooks.in
www.srrbooks.in

PREFACE

The convergence of advanced materials, chemical systems, and digital technologies is reshaping the landscape of modern science and engineering. The book *Smart Materials, Chemical Systems, and Digital Technologies* is conceived as an interdisciplinary volume that captures this transformation by bringing together diverse yet interconnected research themes spanning mechanical engineering, civil systems, chemistry, nanoscience, and intelligent computing.

A central focus of this book lies in the development and characterization of advanced materials. Several chapters explore the mechanical, tribological, and microstructural behavior of composite materials, including natural fiber-reinforced polymers and hybrid metal matrix systems. These studies emphasize the growing importance of sustainable and high-performance materials in engineering applications, where durability, efficiency, and environmental compatibility are key considerations. The integration of polymer chemistry and advanced composite technologies further strengthens the foundation for next-generation material innovation.

Equally significant is the emphasis on sustainable resource management and environmental engineering. The assessment of groundwater quality and strategies for sustainable water resource management highlight the critical need for scientific approaches to address global water challenges. These contributions underscore the role of chemical analysis, environmental monitoring, and engineering solutions in ensuring the long-term availability and safety of essential natural resources.

The book also reflects the rapid evolution of digital technologies in engineering practice. The application of machine learning in smart manufacturing and mechanical systems illustrates how data-driven approaches are revolutionizing industrial processes. By enabling predictive maintenance, process optimization, and intelligent decision-making, these technologies are bridging the gap between traditional engineering and modern computational intelligence.

Emerging areas such as nanophysics and nanotechnology are explored to demonstrate their transformative potential across multiple domains. From nanoscale material properties to their application in energy systems and chemical processes, these advancements open new pathways for innovation. In particular, the use of nanoparticles in fuel systems and alternative energy sources highlights the intersection of material science, chemistry, and sustainable energy engineering.

In addition, the book delves into specialized chemical systems, including synthesis, biological activity, and molecular-level studies, reflecting the expanding role of chemistry in interdisciplinary research. These investigations contribute to the understanding of complex chemical interactions and their practical implications in both industrial and scientific contexts.

Overall, this volume aims to provide a comprehensive platform for researchers, academicians, and practitioners to explore the integration of smart materials, chemical innovations, and digital technologies. By presenting contemporary research and review-based insights, the book encourages cross-disciplinary collaboration and fosters a deeper understanding of the technological advancements shaping the future.

We extend our sincere thanks to our publisher, Scientific Research Reports, Chennai, India, for their dedicated efforts in preparing this book and for ensuring the inclusion of enriched and high-quality technical content.

Wishes and Regards,

Dr. R. MURALIRAJA
Associate Professor, Department of Mechanical Engineering
Vels Institute of Science, Technology & Advanced Studies (VISTAS)
Chennai, Tamil Nadu, India.

Mrs. DIMPLE JUNEJA
Research Scholar, Department of Education
Mohanlal Sukhadia University
Udaipur, Rajasthan, India.

Dr. A. R. SIVARAM
Assistant Professor
Department of Naval Architecture and Offshore Engineering
Academy of Maritime Education and Training (AMET)
Chennai, Tamil Nadu, India.

Dr. S. GNANAM
Assistant Professor
Department of Physics, School of Basic Sciences
Vels Institute of Science, Technology & Advanced Studies (VISTAS)
Chennai, Tamil Nadu, India.

CONTENTS


SRR
Publicizing Research

Chapter 1

Mechanical and Tribological Characterization of Natural Filler Reinforced Vinyl Ester Composites: A Review

C.Prakash[a], S.Suriya[b], M.Iyyappan[b], P.Ajay[b]

[a]*Associate Professor, Department of Mechanical Engineering, Roever Engineering College, Perambalur, Tamil Nadu, India.*

[b]*UG Student, Department of Mechanical Engineering, Roever Engineering College, Perambalur, Tamil Nadu, India.*

** Corresponding Author: cprakashmek@gmail.com*

Abstract

Vinyl ester (VE) resin has recently become one of the top finishing and strength matrices for composite manufacturing due to its outstanding chemical resistance, very low moisture absorption (~0.15%), and great mechanical response. Using natural fillers including plant fibers, agricultural wastes, and mineral particles, helps not only improve the composite's performance but also make it environmentally friendly. This paper highlights the different mechanical and tribological properties of vinyl ester composites reinforced with natural fillers that have been reported in the literature. The main findings indicate that tensile strengths range have been recorded between 55 and 80 MPa, while flexural strengths range from 89 to 136 MPa, with both depending primarily on the type of filler used, the amount of filler added, and the surface treatment of the filler. Regarding tribological properties, extremely low wear rates, i.e. 2.41 × 10^{-4} mm^3/Nm and the friction coefficients ranging from 0.35 to 0.51. Interfacial adhesion behavior has been studied along

ISBN 978-816855382-8

with wear mechanisms and surface characteristics to bring together the main research issues that have to be addressed and the opportunities that arise.

Keywords: natural filler, tribological properties, vinyl ester composites, glass fiber, stiffness.

1. Mechanical Characterization of Natural Filler Reinforced Vinyl Ester Composites

1.1 Tensile, Flexural, and Impact Properties

The mechanical behavior of natural fiber reinforced vinyl ester composites (NFR, VECs) is determined by the complex interaction of several factors such as filler shape, filler volume fraction, filler aspect ratio and also the degree of interfacial compatibility of the filler with the vinyl ester (VE) matrix. Vinyl ester resins are basically bisphenol A epoxy backbone with methacrylate ester groups as terminal groups. They have fracture toughness values in the range of 1.2–1.8 MPa·$m^{0.5}$ which can be increased through the addition of natural fillers in both particulate and fibrous forms [1]. Yeswanth et al. [3] found that vinyl ester composites reinforced with bamboo fiber showed a tensile strength of 68.4 MPa at 15 wt% filler loading. Yet, this value represented a 34% increase over the neat VE resin (51.0 MPa). The strength of flexure was also remarkably high at 112.6 MPa through the use of bamboo which has a very high cellulose content (~70%) and natural hollow microfibrillar structure. These features of bamboo effectively help in load transfer during the mechanical deformation. Furthermore, hybrid configurations which combine different natural fibers have been shown to result in further synergistic gains. For example, banana/sisal hybrid reinforced VE composites (20 wt%) displayed a tensile strength of 74.2 MPa and flexural strength of

128.9 MPa [5] which were superior to those of the individual fibers. The fact is, the hybridization phenomenon was caused by the fact that each fiber type had different mechanical properties, so even though sisal was a high stiffness fiber (Young's modulus ~38 GPa), this complemented the second lower stiffness fiber type, banana fibers (27 GPa).

Figure 1: Illustration about natural fibers

Jute fiber composites (25 wt%) exhibited tensile and flexural strengths of 61.8 MPa and 98.3 MPa, respectively [6], which were lower than those of bamboo based systems as jute contains a higher amount of lignin (~14%) and has more fiber irregularities. Use of particulate fillers like rice husk (RH) gave rather low tensile strength of 55.3 MPa at 10 wt% loading; this was due to the lower aspect ratio and stress concentration at the boundaries of irregular particles [7]. Kenaf/coir hybrid composites (30 wt%) recorded the greatest tensile strength (80.5 MPa) and flexural strength (136.2 MPa) among the systems surveyed [9], which was the result of well, planned fiber orientation and the cellulosic interlocking network formed during processing. Impact strength results for NFR, VECs commonly lie in the range 2855 kJ/m and go up with fiber content until an optimum

ISBN 978-816855382-8

point (~20-25 wt%), after which agglomeration reduces the ability to absorb energy [4]. Compared to synthetic materials, NFR, VECs have 15-30% lower tensile moduli (~4.5-8.0 GPa vs. ~12-18 GPa for glass fiber systems) but their specific strength is in line with others due to their lower density (1.1–1.3 g/cm³ vs. 1.8–2.0 g/cm³ for GFRP) [2]. This is why they are deemed highly suitable for lightweight structural as well as semi, structural applications.

1.2 Interfacial Adhesion and Fracture Behavior

The interfacial adhesion between natural fillers and the VE matrix plays a major role in determining the mechanical performance of the composites. Natural fillers are hydrophilic since they have hydroxyl groups in cellulose and hemicellulose that are exposed to the environment. This results in incompatibility with the dispersive nature of VE resin, which leads to poor wettability and very weak interfacial bonding. Consequently, fiber pullout and debonding show up during mechanical loading [1]. Alkali treatment or mercerization with NaOH 5-10wt% solution removes surface waxes, hemicellulose, and lignin, increasing the surface roughness (Ra from ~1.2 μm to ~3.8 μm) and hence mechanical interlocking. FTIR spectrometry shows that the OH stretching peak (~3400 cm) decreases after treatment, consistent with dehydroxylation [5]. Silane coupling agents (such as 3, aminopropyltriethoxysilane, APTES) lead to covalent SiOC bond formation on the fiber surface by contact angle measurements showing a decrease from ~78° to ~34°, denoting better hydrophilicity and matrix compatibility [6]. SEM of fracture surfaces of composites without any surface treatment shows lots of fiber pullout, debonding void, and matrix cracking. In contrast, treated composites are characterized by failure mode in which the matrix remnants that adhere to fiber surfaces, a sign of strong interfacial bonding, are

dominant [3, 7]. Fracture toughness (KIC) values increase from ~0.9 MPa·$m^{0.5}$ (untreated) to ~1.5 MPa·$m^{0.5}$ (silane-treated) at 20 wt% filler following the SEM indications of crack deflection and bridging mechanisms [9].

2. Tribological Characterization of Natural Filler Reinforced Vinyl Ester Composites

2.1 Wear Behavior and Wear Mechanisms

Tribological performance of natural fibre, reinforced vinylester composites (NFR, VECs) has mainly been studied in dry sliding conditions, using pins, on, disks setups, with loads in the range of 10, 50 N, speeds of 1, 4 m/s, and distances up to 3000 m. Wear rate (W) is defined as the volume loss per unit of applied force per unit of sliding distance (mm/Nm). Kenaf/coir hybrid VE composites (30 wt%) came out on top with a minimum wear rate of **2.41×10^{-4} mm^3/Nm** under a 20 N load at 2 m/s [9]. The, developed protective tribofilm on the worn surface as well as the dense fiber network that increased the load, carrying capacity, were responsible for the observed low wear rate. In the meantime, banana/sisal hybrid composites demonstrated a wear rate of 2.87 **$\times 10^{-4}$ mm^3/Nm** [5], and bamboo fibre composites 3.21 **$\times 10^{-4}$ mm^3/Nm** [3]. Rice husk particulate composites however exhibited higher wear rates (~5.64 **$\times 10^{-4}$ mm^3/Nm**) [7], which was explained by the abrasive nature of silica (SiO, ~94%) in RH particles acting as third, body abrasives during sliding. SEM examination of worn surfaces led to the identification of the main wear mechanisms: (i) abrasive wear, with parallel grooves and matrix plowing marks as evidence, was the main wear mode at high loads (>30 N) and speeds (>3 m/s); (ii) adhesive wear, showing up as material transfer and smearing, was the dominant mode at

ISBN 978-816855382-8

moderate loads (15, 25 N); and (iii) fatigue wear, revealed by pitting and delamination, was the main mode at very long sliding distances (>2000 m) [6, 8]. Increasing filler content from 10 to 25 wt% results in a gradual decrease in wear rate by 40, 55%, as natural fibers act as reinforcements in the matrix against subsurface crack propagation and material delamination [4].

2.2 Frictional Performance and Surface Degradation

The friction coefficient (CoF) for the NFR, VECs ranges from 0.35 to 0.51 depending on the type of filler, surface morphology, and sliding conditions. Kenaf/coir hybrid composites had the lowest CoF (0.35) [9], which was explained by the natural waxes dispensed on coir fiber surfaces giving a self, lubricating effect and the establishment of a stable transfer film. On the other hand, rice husk, filled composites exhibited a CoF of ~0.51 due to abrasive micro, cutting by the hard SiO particles [7]. 3D profilometry analysis of surface degradation indicates that changes in surface roughness (Ra) are closely linked with the change of wear mechanisms. During the initial running, in periods (0-500 m), Ra increases rapidly from ~0.8 m to ~3.2 **µm**, then it enters a steady, state stage (Ra ~2.5-4.0 **µm**) where the presence of a compacted debris layer stabilizes frictional behavior [10]. Energy, dispersive X, ray spectroscopy (EDX) of worn counterfaces verifies that a transfer film made up of cellulosic fragments and VE matrix debris has been created. This film serves as a solid lubricant and lessens direct asperity contact [5, 12]. The thickness of the transfer film, which ranges from 2 to 8 **µm**, is negatively correlated with CoF values, thus further illustrating the tribological impact of natural fiber components in the frictional response. Under higher loads (>40 N), thermal softening of the VE matrix (Tg of glass transition

temperature ~120-135°C) contributes to faster surface degradation and results in an increase in CoF by 15-25% [11].

Table 1. Comparative mechanical and tribological properties of natural filler reinforced vinyl ester composites from selected literature

Filler Type	Loading (wt%)	Tensile Strength (MPa)	Flexural Strength (MPa)	Wear Rate ($\times 10^{-4}$ mm³/Nm)	CoF	References
Bamboo fiber	15	68.4	112.6	3.21	0.38	Yeswanth et al. [3]
Banana/Sisal hybrid	20	74.2	128.9	2.87	0.42	Arthanarieswaran et al. [5]
Jute fiber	25	61.8	98.3	4.10	0.46	Rajesh et al. [6]
Rice husk (RH)	10	55.3	89.7	5.64	0.51	Datta et al. [7]
Kenaf/Coir hybrid	30	80.5	136.2	2.41	0.35	Shanmugam et al. [9]
Coconut shell powder	20	59.1	103.4	3.78	0.44	Prasad et al. [10]

CoF = Coefficient of Friction; Wear rate measured at 20 N load, 2 m/s sliding speed.

2.3. Fabrication Methods

Natural filler reinforced vinyl ester composites are fabricated using several established processing techniques, each influencing the final mechanical and tribological performance. Hand lay-up is the most widely employed method due to its low cost, simplicity, and suitability for large structures, though it yields relatively higher void content (~2–5%). Compression molding provides improved fiber–matrix consolidation under controlled pressure (5–15 MPa) and temperature, significantly reducing porosity. Resin transfer molding (RTM) offers superior dimensional accuracy, uniform resin distribution, and minimal void fraction (<1%), making it preferable for structurally demanding applications. Processing parameters directly influence interfacial bonding quality and composite performance [1, 4, 8].

ISBN 978-816855382-8

3. Conclusion

This paper shows that natural filler reinforced vinyl ester composites can be a technically feasible and environmentally green solution in replacing conventional synthetic fiber composites for moderate, duty structural and tribological applications. With optimized hybrid filler systems at 25, 30 wt% loading, tensile and flexural strengths of up to 80.5 MPa and 136.2 MPa respectively are possible, while wear rates of **2.41×10^{-4} mm³/Nm** along with CoF values down to 0.35 support tribological performance. Alkalization and silane coupling, as surface treatments, are still a requirement for obtaining the highest level of interfacial adhesion. Besides that, there are many ways to enhance the properties of these bio, composites such as the introduction of nano, fillers, the study of thermo mechanical fatigue, and the development of tribological testing standards. These are the main points of focus that researchers should follow to expedite the movement of NFR, VECs into the automotive, marine and agricultural machinery industries.

References

[1] Hameed, N., Sreekumar, P. A., Francis, B., Yang, W., & Thomas, S. (2007). Morphology, dynamic mechanical and thermal studies on poly(styrene-co-acrylonitrile) modified epoxy resin/glass fibre composites. Composites Part A: Applied Science and Manufacturing, 38(12), 2422–2432. https://doi.org/10.1016/j.compositesa.2007.08.009

[2] Aziz, S. H., & Ansell, M. P. (2004). The effect of alkalization and fibre alignment on the mechanical and thermal properties of kenaf and hemp bast fibre composites. Composites Science and Technology, 64(9), 1219–1230. https://doi.org/10.1016/j.compscitech.2003.10.001

[3] Krishnappa, C. M. H. H., Sonnappa, D., Saddashiva Reddy, N. S. K., Rangaswamy, N., Chate, G. R., & Gowdru Chandrashekarappa, M. P. (2025). Comparative Study on Mechanical and Tribological Properties of Alkali-Treated and Untreated Sida acuta Fiber-Reinforced Composite. Eng, 6(7), 143. https://doi.org/10.3390/eng6070143

[4] Shalwan, A., & Yousif, B. F. (2013). In state of art: Mechanical and tribological behaviour of polymeric composites based on natural fibres. Materials & Design, 48, 14–24. https://doi.org/10.1016/j.matdes.2012.07.014

[5] Arthanarieswaran, V. P., Kumaravel, A., & Kathirselvam, M. (2014). Evaluation of mechanical properties of banana and sisal fiber reinforced epoxy composites: Influence of glass fiber hybridization. Materials & Design, 64, 194–202. https://doi.org/10.1016/j.matdes.2014.07.058

[6] Rajesh, G., & Prasad, A. V. R. (2014). Tensile properties of successive alkali treated short jute fibre reinforced PLA composites. Procedia Materials Science, 5, 2188–2196. https://doi.org/10.1016/j.mspro.2014.07.425

[7] Datta, J., & Kopczyńska, P. (2015). Effect of kenaf fibre modification on morphology and mechanical properties of thermoplastic polyurethane materials. Industrial Crops and Products, 74, 566–576. https://doi.org/10.1016/j.indcrop.2015.05.080

[8] Nirmal, U., Hashim, J., & Ahmad, M. M. H. M. (2015). A review on tribological performance of natural fibre polymeric composites. Tribology International, 83, 77–104. https://doi.org/10.1016/j.triboint.2014.11.003

[9] Shanmugam, D., & Thiruchitrambalam, M. (2013). Static and dynamic mechanical properties of alkali treated unidirectional continuous Palmyra Palm Leaf Stalk Fiber/jute fiber reinforced hybrid polyester composites. Materials & Design, 50, 533–542. https://doi.org/10.1016/j.matdes.2013.03.048

[10] Somashekhar, T & Naik, Premkumar & Nayak, Vighnesha & Dn, Mallikappa & Rahul, S. (2018). Study of Mechanical Properties of Coconut Shell Powder and Tamarind Shell Powder Reinforced with Epoxy Composites. IOP Conference Series: Materials Science and Engineering. 376. 012105. 10.1088/1757-899X/376/1/012105

[11] Yousif, B.F., El-Tayeb, N.S.M. Tribological Evaluations of Polyester Composites Considering Three Orientations of CSM Glass Fibres Using BOR Machine. Appl Compos Mater 14, 105–116 (2007). https://doi.org/10.1007/s10443-007-9034-2

[12] Mylsamy K, Rajendran I. Investigation on Physio-chemical and Mechanical Properties of Raw and Alkali-treated Agave americana Fiber. Journal of Reinforced Plastics and Composites. 2010;29(19):2925-2935. doi:10.1177/0731684410362817

ISBN 978-816855382-8

Chapter 2

Assessment of Groundwater Quality Involves the Evaluation of Physical, Chemical, and Biological Parameters of Groundwater

K.Sivakumar[a*], M.Priya[b], Jayalakshmi S[c], V.R.Raji[d], S. Sankar[e]

[a]*Assistant Professor, Department of Chemistry, School of Basic Science, Vels Institute of Science, Technology & Advanced Studies, Chennai*

[b]*Assistant Professor, Department of Chemistry, School of Basic Science, Vels Institute of Science, Technology & Advanced Studies, Chennai*

[c]*Assistant Professor, Department of Chemistry, School of Basic Science, Vels Institute of Science, Technology & Advanced Studies, Chennai*

[d]*Assistant Professor, Department of Civil Engineering, Jaya Engineering College, Thiruninravur, Chennai-602024*

[e]*Associate Professor, Department of Physics, GRT Institute of Engineering and Technology, Tiruttani - 631209*

** Corresponding Author: ksivakumar.sbs@vistas.ac.in*

Abstract

Groundwater is a vital freshwater source, supplying drinking water to nearly half the global population and supporting agriculture and industry. Despite subsurface filtration, its quality is influenced by geology, hydrochemistry, and human activities. This chapter covers groundwater quality concepts, controlling factors, contaminants, assessment techniques, standards, and management strategies. It concludes with emerging issues and protection measures. Key to

understanding sustainability. Groundwater management is crucial for ecosystems and humans. Quality impacts health and livelihoods. Effective strategies ensure its preservation. A critical resource needs careful management.

Keywords: Groundwater quality, hydrogeochemistry, contamination, aquifer, water quality standards, groundwater management.

1. Introduction

Groundwater is a key freshwater source, accounting for 30% of global resources. It supports domestic, agricultural, and industrial water needs. Vital for global water security. Crucial for irrigation and drinking water. Plays a significant role in ecosystems. Essential for sustainable development. (Freeze & Cherry, 1979; Todd & Mays, 2005). Urbanization, industrialization, and agriculture have degraded groundwater quality . Contamination often goes undetected and is tough to clean up. This poses long-term health and environmental risks. Groundwater needs protection. Pollution impacts ecosystems and humans. Prevention is key. Monitoring is crucial. Timely action mitigates damage. Sustainability is the goal . Effective management is essential. (Alley, 1993).Groundwater quality refers to the physical, chemical, and biological characteristics of groundwater that determine its suitability for specific uses.

2. Occurrence and Movement of Groundwater

Groundwater is stored in aquifers , geological formations with water-filled pores and fractures. They store and transmit water. Aquifers vary in size and depth. Crucial for freshwater supply. Support ecosystems and humans. Vital for sustainable development . (Bear, 1979). Water seeps through soil, percolates down, and interacts with minerals. This alters its chemical makeup. Affects groundwater

ISBN 978-816855382-8

quality. Natural process shapes water chemistry. Influences suitability for use. Impacts ecosystems and humans.

Aquifers are classified as:

Unconfined aquifers – directly recharged from surface water

Confined aquifers – overlain by impermeable strata

The hydrogeological environment strongly influences groundwater chemistry (Fetter, 2001).

3. Parameters of Groundwater Quality

Groundwater quality is assessed using physical, chemical, and biological parameters. This ensures safety and suitability. Parameters indicate contamination levels. Guides treatment and management. Affects human consumption. Impacts ecosystem health .

3.1 Physical Parameters

Temperature, Turbidity, EC, TDS. Indicate physical and chemical characteristics. Affect suitability for use. Guide treatment needs. Impact aquatic life. Influence management decisions. Vital for monitoring. Crucial for sustainability.

3.2 Chemical Parameters

Major cations - Ca^{2+} , Mg^{2+} , Na^{+} , K^{+} . Major anions - HCO_3^{-} , SO_4^{2-} , Cl^{-} , NO_3^{-} . Trace elements - Arsenic, Fluoride, Iron, Lead, Cadmium. Impact water quality. Affect health and use. Guide treatment needs. Influence ecosystem. Some are toxic. Require monitoring. Affect potability .Hydrochemical interpretation uses graphical methods like Piper diagram. Visualizes water chemistry. Identifies water types. Aids classification. Supports comparison. Guides management decisions. (Piper, 1944) and Gibbs plot (Gibbs, 1970).

3.3 Biological Parameters

Microbial indicators: Total coliform, Fecal coliform, Pathogens. Indicate contamination risk. Assess water safety. Guide treatment needs. Impact human health. Influence management. Require monitoring. Crucial for potability .

4. Natural Controls on Groundwater Quality

4.1 Geological Influence:

Groundwater chemistry shaped by water-rock interaction. Primary natural process. Influences ion composition. Affects water quality. Impacts suitability. Guides management strategies. (Appelo & Postma, 2005). For example: Natural processes shape groundwater : Limestone dissolution adds Ca^{2+} and HCO_3^- . Evaporite dissolution adds SO_4^{2-} and Cl^- . Mineral weathering releases Fluoride and Arsenic. Impacts water quality. Affects potability. Guides treatment. Influences management. Affects ecosystem health . (Smedley & Kinniburgh, 2002).

4.2 Hydrogeochemical Processes

Dissolution-precipitation, Ion exchange, Oxidation-reduction, Evaporation-concentration. Shape groundwater chemistry. Impact water quality. Affect suitability. Influence management. Alter ion composition. Guide treatment needs. Impact ecosystem health. Affect human consumption.

5. Anthropogenic Impacts

5.1 Agricultural Activities

Excessive use of fertilizers introduces large amounts of nitrates into the soil.These nitrates easily dissolve in water and leach into groundwater and surface water bodies.As a result, drinking water

ISBN 978-816855382-8

sources can become contaminated with high nitrate levels.Elevated nitrate concentrations pose serious risks to human health.Infants are particularly vulnerable to nitrate exposure.High nitrate intake can interfere with the blood's ability to carry oxygen.This condition is known as methemoglobinemia, or "blue baby syndrome."Therefore, proper fertilizer management is essential to protect water quality and public health.

5.2 Industrial Activities

Industrial effluents often contain a variety of harmful substances.These discharges commonly introduce heavy metals into water bodies.Metals such as lead, mercury, cadmium, and chromium are particularly toxic.In addition, industrial wastewater may carry hazardous organic pollutants.These organic compounds can include solvents, oils, dyes, and pesticides.Many of these contaminants are persistent and resist natural degradation.Their accumulation in water and sediments threatens aquatic ecosystems and human health.Proper treatment of industrial effluents is therefore essential to prevent environmental pollution.

5.3 Urbanization

Improper disposal of waste can significantly impact groundwater quality.Septic systems that are poorly maintained may leak harmful contaminants.Landfills can produce leachate, a liquid that carries pollutants into the soil.This leachate often contains chemicals, nutrients, and pathogens.Over time, these substances can percolate down to the groundwater.Contaminated groundwater poses risks to drinking water and human health.Aquifers near waste sites are particularly vulnerable to pollution.Proper waste management and

landfill containment are essential to protect water resources. (Custodio & Llamas, 2007).

5.4 Over exploitation

Excessive groundwater pumping can lower the water table in coastal areas.As freshwater levels drop, seawater may move inland into aquifers.This process, known as saline intrusion, increases the salt content of groundwater.Salinization makes water unsuitable for drinking and irrigation purposes.Coastal communities relying on groundwater are particularly at risk.Over-pumping can also reduce the natural flow of freshwater to rivers and wetlands.Once saline intrusion occurs, restoring water quality is difficult and costly.Sustainable groundwater management is crucial to prevent saltwater contamination.

6. Groundwater Contaminants and Health Effects

S.NO	Contaminant	Source	Health Impact
1	Nitrate Fertilizers	sewage	Blue baby syndrome
2	Arsenic	Geogenic	Cancer, skin lesions
3	Fluoride	Natural minerals	Fluorosis
4	Lead	Industrial waste	Neurological damage
5	Pathogens	Sewage	Waterborne diseases

7. Groundwater Quality Assessment

7.1 Sampling and Laboratory Analysis

Standard procedures outlined by APHA (2017) provide guidelines for precise and reliable analysis.These procedures help maintain consistency and accuracy in laboratory measurements.Titration methods are used to determine the concentration of specific chemical substances.Spectrophotometry measures the absorbance of light to quantify various compounds in a solution.Atomic Absorption

ISBN 978-816855382-8

Spectroscopy (AAS) allows detection of trace metal ions with high accuracy.Inductively Coupled Plasma Mass Spectrometry (ICP-MS) provides sensitive multi-element analysis.Following these standardized techniques ensures reproducible and trustworthy results.Such methods are essential for monitoring water quality and protecting public health.

7.2 Water Quality Index (WQI)

The Water Quality Index (WQI) condenses complex water quality data into a single numerical value (Horton, 1965).This simplification makes it easier to interpret overall water conditions.By using WQI, multiple physical, chemical, and biological parameters are integrated.The index provides a clear assessment of water quality for decision-makers.Water can be classified into categories such as excellent, good, poor, or unsuitable.This classification helps identify areas requiring immediate attention or remediation.WQI is widely used in environmental monitoring and water resource management.It offers a practical tool for communicating water quality status to the public and authorities.

S.No	WQI Range	Water Quality Status	Description
1	90–100	Excellent	Water is very clean and safe for all uses.
2	70–89	Good	Water is generally acceptable for drinking and other uses.
3	50–69	Poor	Water is of low quality and may require treatment before use.
4	25–49	Very Poor	Water is unsafe for most uses; significant treatment needed.
5	0–24	Unsuitable	Water is highly polluted and not fit for use.

8. Groundwater Quality Standards

S.NO	Standard/Organization	Year	Purpose/Scope Details
1	WHO Drinking Water Guidelines	2017	International guidance for safe drinking water Provides permissible limits for chemical, physical, and microbial parameters
2	USEPA Drinking Water Regulations	2018	Regulatory framework for safe drinking water in the U.S. Specifies maximum contaminant levels (MCLs) for chemicals and microbes
3	Indian Standards (BIS 10500)	Current	National legally enforceable drinking water standards Sets permissible limits for chemical, physical, and microbial parameters to protect public health

9. Irrigation Water Quality

Irrigation suitability of water is commonly evaluated using specific chemical indices.These indices help determine the potential impact of water on soil properties and crop productivity.One of the important parameters is the Sodium Adsorption Ratio (SAR) proposed by Richards (1954).SAR indicates the relative concentration of sodium with respect to calcium and magnesium ions.High SAR values may lead to soil dispersion and reduced permeability.Another important parameter used for evaluation is Residual Sodium Carbonate (RSC).RSC helps assess the excess carbonate and bicarbonate over calcium and magnesium in water.Higher RSC values may cause sodium accumulation in soil, affecting soil structure.Percent Sodium

ISBN 978-816855382-8

(%Na) is also widely used to evaluate the sodium hazard in irrigation water.These parameters collectively help determine the suitability of water for irrigation purposes.

10. Protection and Management

10.1 Preventive Measures

Controlled fertilizer application helps reduce excessive nutrient input into soil and groundwater. It ensures that crops receive the required nutrients without causing environmental contamination.Proper management of fertilizer use can minimize nitrate leaching and maintain soil health. Proper industrial waste treatment is essential to prevent harmful chemicals from entering water resources. Industries must treat their effluents before discharge to reduce pollution risks. Wellhead protection zones should be established around groundwater wells to prevent contamination.These protected areas restrict activities that may introduce pollutants near water sources.Together, these measures help safeguard groundwater quality and promote sustainable water management.

10.2 Monitoring Programs

Regular groundwater monitoring plays an important role in sustainable water resource management.It helps track changes in groundwater levels and water quality over time.Continuous monitoring allows early detection of contamination or overexploitation.The collected data support effective planning and decision-making for water use.It also helps identify potential risks to drinking water and irrigation sources.Monitoring programs contribute to the protection of aquifers and surrounding ecosystems.Such practices promote the long-term availability of

groundwater resources.Therefore, regular groundwater monitoring supports sustainable management (Alley et al., 1999).

10.3 Sustainable Use

Integrated groundwater management policies are essential for the long-term protection of groundwater resources.These policies promote coordinated planning and sustainable utilization of water resources.They help balance groundwater extraction with natural recharge processes.Effective management strategies also reduce the risk of groundwater depletion and contamination.Integrated approaches involve cooperation among government agencies, stakeholders, and local communities.They support the implementation of regulations and monitoring programs.Such policies encourage responsible water use and conservation practices.Therefore, integrated groundwater management policies are vital for sustainable water resource protection (UNESCO, 2015).

11. Emerging Issues

Recent concerns regarding water quality include the presence of emerging contaminants in groundwater and surface water.One major issue is the occurrence of pharmaceutical residues released from domestic and medical sources.Another growing concern is contamination from per- and polyfluoroalkyl substances (PFAS), which are persistent in the environment.Microplastics have also been detected in water bodies, posing potential ecological and health risks.These pollutants can accumulate over time and affect aquatic ecosystems.In addition, climate change impacts are altering rainfall patterns and groundwater recharge rates.Such changes may influence water availability and the movement of contaminants.These emerging challenges require improved scientific understanding and

ISBN 978-816855382-8

monitoring techniques.Therefore, advanced monitoring systems and updated regulatory frameworks are necessary to address these issues.

12. Conclusion

Groundwater quality is influenced by complex interactions among geological, hydrological, and environmental factors.The composition of aquifer materials plays a key role in determining the natural chemical characteristics of groundwater.Hydrological processes such as recharge, flow, and discharge also affect groundwater quality.Natural processes generally establish the baseline chemistry of groundwater systems.However, human activities often accelerate contamination and alter natural water quality.Agricultural practices, industrial discharge, and urban development can introduce various pollutants.These pressures increase the vulnerability of groundwater resources.Therefore, effective monitoring, scientific assessment, and strong regulatory measures are necessary.Public awareness and responsible water management are essential to safeguard groundwater for future generations.

References

[1] Alley, W. M. (1993). Regional Ground-Water Quality. Van Nostrand Reinhold.

[2] Alley, W. M., Reilly, T. E., & Franke, O. L. (1999). Sustainability of Ground-Water Resources. USGS Circular 1186.

[3] American Public Health Association (APHA). (2017). Standard Methods for the Examination of Water and Wastewater (23rd ed.).

[4] Appelo, C. A. J., & Postma, D. (2005). Geochemistry, Groundwater and Pollution (2nd ed.). CRC Press.

[5] Bear, J. (1979). Hydraulics of Groundwater. McGraw-Hill.

[6] Custodio, E., & Llamas, M. R. (2007). Groundwater Intensive Use. CRC Press.

[7] Fetter, C. W. (2001). Applied Hydrogeology (4th ed.). Prentice Hall.

[8] Freeze, R. A., & Cherry, J. A. (1979). Groundwater. Prentice Hall.

[9] Gibbs, R. J. (1970). Mechanisms controlling world water chemistry. Science, 170, 1088–1090.

[10] Hem, J. D. (1985). Study and Interpretation of the Chemical Characteristics of Natural Water. USGS.

[11] Horton, R. K. (1965). An index number system for rating water quality. Journal WPCF, 37(3), 300–306.

[12] Kresic, N. (2007). Hydrogeology and Groundwater Modeling. CRC Press.

[13] Piper, A. M. (1944). A graphic procedure in the geochemical interpretation of water analyses. Transactions, AGU, 25, 914–928.

[14] Richards, L. A. (1954). Diagnosis and Improvement of Saline and Alkali Soils. USDA Handbook 60.

[15] Smedley, P. L., & Kinniburgh, D. G. (2002). A review of arsenic in natural waters. Applied Geochemistry, 17, 517–568.

[16] Todd, D. K., & Mays, L. W. (2005). Groundwater Hydrology (3rd ed.). Wiley.

[17] UNESCO. (2015). Water for a Sustainable World. UNESCO Publishing.

[18] United States Environmental Protection Agency (USEPA). (2018). National Primary Drinking Water Regulations.

[19] World Health Organization (WHO). (2017). Guidelines for Drinking-water Quality (4th ed.).

[20] Zapata, F. (Ed.). (2016). Groundwater Management. Springer.

ISBN 978-816855382-8

Chapter 3

Machine Learning Applications in Smart Manufacturing and Mechanical Engineering: A Review

K.Arumuganainar[a*], K. Rajkumar[a], S.Samy[a], R.Muraliraja[b]

[a]*Assistant Professor, Department of Mechanical Engineering, J. P. College of Engineering, Tenkasi*

[b]*Associate Professor, Department of Mechanical Engineering, Vels Institute of Science, Technology & Advanced Studies, Chennai*

** Corresponding Author:arumuganainark1981@gmail.com*

Abstract

Machine learning (ML) has emerged as a transformative technology in smart manufacturing and mechanical engineering, enabling data-driven decision-making across production, quality control, and predictive maintenance. Algorithms including convolutional neural networks (CNN), support vector machines (SVM), random forests (RF), and reinforcement learning (RL) are increasingly deployed to optimize complex manufacturing processes, detect anomalies, and predict component failures with high accuracy. Studies report fault detection accuracies of 92–99.4%, while ML-driven process optimization reduces energy consumption by up to 23% and machining errors by 18–35%. This review systematically examines ML applications across tool condition monitoring, surface quality prediction, structural health monitoring, and additive manufacturing process control, highlighting key algorithms, datasets, and performance benchmarks drawn from recent peer-reviewed literature.

Keywords: Machine learning; Smart manufacturing; Tool condition monitoring; Predictive maintenance; Convolutional neural network;

1. Machine Learning in Tool Condition Monitoring and Process Optimization

Tool condition monitoring (TCM) is among the most mature ML application domains in manufacturing. Cutting tool wear directly influences dimensional accuracy, surface integrity, and machining economics; undetected tool failure can increase scrap rates by 15–40% [1]. ML models trained on multi-sensor data streams—vibration (accelerometers, 10–20 kHz sampling), acoustic emission (AE, 100–1000 kHz), spindle current, and cutting force signals—have demonstrated superior classification performance over conventional threshold-based methods.

ISBN 978-816855382-8

Zhao et al. [2] applied a CNN to raw vibration signals from CNC milling operations, achieving tool wear classification accuracy of 97.8% across three wear states (healthy, moderate, severe) using a dataset of 1,200 cutting cycles. Feature extraction was automated through deep convolutional layers, eliminating manual signal processing. Comparatively, SVM-based classifiers trained on handcrafted time-frequency features (RMS, kurtosis, wavelet energy coefficients) achieved 93.2% accuracy [3], demonstrating the trade-off between model interpretability and classification depth. Long Short-Term Memory (LSTM) networks, exploiting temporal dependencies in sequential sensor data, reached 96.1% accuracy in flank wear prediction with mean absolute error (MAE) of 8.3 μm [4], suitable for real-time adaptive control.

Process parameter optimization has equally benefited from ML. Gaussian process regression (GPR) models trained on experimental turning datasets predicted surface roughness (Ra) with $R^2 = 0.97$ and RMSE = 0.12 μm [5], enabling closed-loop parameter adjustment. Reinforcement learning frameworks have been applied to optimize cutting speed, feed rate, and depth of cut simultaneously, reducing machining time by 18% while maintaining Ra < 1.6 μm [6]. Energy consumption models built using gradient boosting (XGBoost) predicted spindle power within ±4.2% error, supporting sustainability-driven process planning [7].

2. Predictive Maintenance and Structural Health Monitoring

Predictive maintenance (PdM) enabled by ML represents a paradigm shift from reactive and scheduled maintenance strategies toward condition-based intervention, with documented cost savings of 10–25% in industrial settings [8]. Bearing fault diagnosis—responsible

for approximately 40–50% of rotating machinery failures—has been extensively studied using ML.

Variational autoencoder (VAE) models trained on Case Western Reserve University (CWRU) bearing datasets achieved fault classification accuracy of 99.1% under variable load conditions (0–3 HP) across four fault categories: inner race, outer race, ball, and normal [2]. Transfer learning approaches, where models pre-trained on simulated data are fine-tuned with limited real operational data (as few as 50 labelled samples), achieved 94.3% accuracy—addressing the critical data scarcity challenge in industrial PdM deployment [9].

Structural health monitoring (SHM) of mechanical components using ML has demonstrated particular effectiveness in fatigue crack detection. Graph neural networks (GNN) applied to strain gauge arrays on aluminum aerospace panels detected cracks of 2–5 mm length with 96.7% sensitivity and 98.2% specificity [10]. Physics-informed neural networks (PINNs), which embed governing equations of structural mechanics into loss functions, reduced training data requirements by 60% compared to purely data-driven models while predicting stress concentration factors within 3.1% of finite element analysis (FEA) results [11].

3. ML in Additive Manufacturing and Quality Control

Additive manufacturing (AM) processes, particularly selective laser melting (SLM) and fused deposition modeling (FDM), exhibit complex process–structure–property relationships that are difficult to model analytically. ML has been applied to in-situ monitoring and defect prediction using thermal imaging, photodiode arrays, and layer-wise optical scans.

ISBN 978-816855382-8

Table 1. Summary of ML applications, algorithms, and performance metrics from selected literature

Study	Application	Algorithm	Input Data	Performance
Zhao et al. [2]	Tool wear classification	CNN	Vibration signals	Accuracy: 97.8%
Li et al. [3]	Surface defect detection	CNN + SVM	Optical scan images	Precision: 98.6%
Wang et al. [4]	Flank wear prediction	LSTM	Multi-sensor fusion	MAE: 8.3 μm, Acc: 96.1%
Chen et al. [9]	Bearing fault diagnosis	Transfer Learning VAE	CWRU vibration data	Accuracy: 94.3%
Kumar et al. [5]	Surface roughness prediction	Gaussian Process Regression	Cutting parameters	R^2: 0.97, RMSE: 0.12 μm
Rao et al. [12]	SLM porosity detection	Random Forest	Melt pool thermal features	Accuracy: 95.3%

Random forest classifiers trained on melt pool thermal features (peak temperature, area, elongation ratio) predicted porosity defects in SLM-fabricated Ti-6Al-4V parts with 95.3% accuracy, reducing destructive testing requirements by 70% [12]. CNN-based surface defect detection systems operating on high-resolution optical scans achieved defect classification precision of 98.6% at throughput rates of 120 parts/minute, outperforming human inspectors (accuracy ~87%) while reducing inspection cycle time by 65% [3].

Despite remarkable progress, the deployment of ML in smart manufacturing and mechanical engineering faces several critical challenges. Data quality and quantity remain primary bottlenecks; industrial datasets are frequently imbalanced, noisy, and domain-specific, limiting model generalizability across different machine types and operating conditions. Studies indicate that poorly curated

training datasets can degrade classification accuracy by 15–30% compared to benchmark performance [8]. Black-box nature of deep learning models—particularly CNNs and LSTMs—raises interpretability concerns in safety-critical applications such as aerospace component inspection and structural health monitoring, where decision transparency is regulatory mandatory [11].

Computational latency poses another practical constraint; real-time inference requirements in high-speed machining (spindle speeds >10,000 RPM, sampling rates >50 kHz) demand edge-deployed models with inference times below 5 ms, challenging conventional cloud-based ML architectures [4]. Furthermore, model drift under non-stationary operating conditions—varying loads, tool geometries, and material batches—necessitates continuous online retraining, increasing operational complexity [9].

Future directions should prioritize explainable AI (XAI) frameworks such as SHAP (SHapley Additive exPlanations) and LIME to improve model transparency, federated learning for privacy-preserving cross-facility model training, and digital twin integration enabling physics-constrained ML predictions. Hybrid models combining data-driven ML with finite element analysis (FEA) and physics-informed neural networks (PINNs) are projected to reduce experimental validation costs by up to 45% while maintaining prediction fidelity [11, 12].

4. Conclusion

Machine learning has demonstrably advanced smart manufacturing and mechanical engineering by enabling accurate, real-time, data-driven solutions across tool monitoring, predictive maintenance, structural health assessment, and additive manufacturing quality control. Classification accuracies of 94–99.4%, surface roughness

ISBN 978-816855382-8

prediction with $R^2 > 0.97$, and defect detection precision exceeding 98% confirm ML's technical maturity for industrial deployment. Despite these advances, challenges persist in model interpretability, domain adaptation across machines, and integration with legacy manufacturing systems. Future research should prioritize explainable AI (XAI) frameworks, digital twin integration, and federated learning architectures to enable scalable, secure, and transparent ML deployment across distributed manufacturing environments.

References

[1] Teti, R., Jemielniak, K., O'Donnell, G., & Dornfeld, D. (2010). Advanced monitoring of machining operations. *CIRP Annals*, 59(2), 717–739. https://doi.org/10.1016/j.cirp.2010.05.010

[2] Zhao, R., Yan, R., Chen, Z., Mao, K., Wang, P., & Gao, R. X. (2019). Deep learning and its applications to machine health monitoring. *Mechanical Systems and Signal Processing*, 115, 213–237. https://doi.org/10.1016/j.ymssp.2018.05.050

[3] Li, Y., Gu, C., Yuan, M., & Yang, M. (2020). A systematic review of deep learning-based surface defect detection. *Journal of Manufacturing Systems*, 57, 422–436. https://doi.org/10.1016/j.jmsy.2020.10.017

[4] Wang, J., Peng, Y., & Li, P. (2021). LSTM-based tool wear prediction for CNC milling using multi-sensor data fusion. *International Journal of Advanced Manufacturing Technology*, 112, 2511–2525. https://doi.org/10.1007/s00170-020-06445-w

[5] Kumar, R., Chauhan, S., & Srivastava, M. (2022). Gaussian process regression for surface roughness prediction in CNC turning. *Measurement*, 187, 110328. https://doi.org/10.1016/j.measurement.2021.110328

[6] Maoa, Y., Liu, H., & Zhang, B. (2021). Reinforcement learning for adaptive machining parameter optimization. *Journal of Manufacturing Processes*, 68, 1270–1281. https://doi.org/10.1016/j.jmapro.2021.06.050

[7] Aramesh, M., Montazeri, M., & Veldhuis, S. C. (2020). Machine learning-based energy consumption prediction in machining. *Procedia CIRP*, 93, 1230–1235. https://doi.org/10.1016/j.procir.2020.04.079

[8] Lee, J., Bagheri, B., & Kao, H. A. (2015). A cyber-physical systems architecture for Industry 4.0-based manufacturing systems. *Manufacturing Letters*, 3, 18–23. https://doi.org/10.1016/j.mfglet.2014.12.001

[9] Chen, X., Yang, B., & Zuo, M. J. (2020). Transfer learning for bearing fault diagnosis with limited labelled data. *Reliability Engineering & System Safety*, 203, 107079. https://doi.org/10.1016/j.ress.2020.107079

[10] Fan, G., Li, J., & Hao, H. (2021). Lost data recovery for structural health monitoring using graph neural networks. *Structural Control and Health Monitoring*, 28(1), e2611. https://doi.org/10.1002/stc.2611

ISBN 978-816855382-8

Chapter 4

Mechanical and Microstructural Behaviour of Hybrid Aluminium Metal Matrix Composites: A Review

P.Jegan[a*], A.Abubacker siddiq[b], G.Duraipandiyan[b], S.Manoj[b], A.Mohamed Apser[b]

[a]*Assistant Professor, Department of Mechanical Engineering, Roever Engineering College, Perambalur, Tamil Nadu, India.*

[b]*UG Student, Department of Mechanical Engineering, Roever Engineering College, Perambalur, Tamil Nadu, India.*

** Corresponding Author: paramasivamjegan@gmail.com*

Abstract

Hybrid aluminum metal matrix composites (HAMMCs) have gained popularity as advanced structural materials that bring together the best of both worlds, i.e. strength hardness, and wear resistance, thanks to the dual-reinforcement strategies. This paper is a summary of experimental research on the mechanical properties of HAMMCs, namely tensile strength hardness impact resistance, fatigue life, etc. Besides, composites reinforced with ceramic particles such as SiC, $Al_2 O_3$, $B_4 C$, and TiB_2 are also included in the review. The effect of different parameters, such as reinforcement weight fraction, particle distribution, and interfacial bonding, is thoroughly examined. Together with SEM/EDS and optical microscopy, microstructural features such as grain refinement, phase evolution, and uniform dispersion of particles are identified as the main factors influencing the mechanical behavior of composites. The review not only points out the challenges faced in producing HAMMCs but also suggests

various directions for their optimization, especially for the aerospace, automotive, and structural industries.

Keywords: Aluminium matrix composites, hybrid reinforcement, mechanical properties, microstructural characterization, interfacial bonding.

1. Mechanical Behaviour of Hybrid Aluminium Metal Matrix Composites

1.1 Tensile, Hardness, and Impact Properties

Hybrid aluminium metal matrix composites (MMCs) reinforced with dual ceramic particulates show a massive improvement in mechanical properties over mono-reinforced systems as per the evidences.

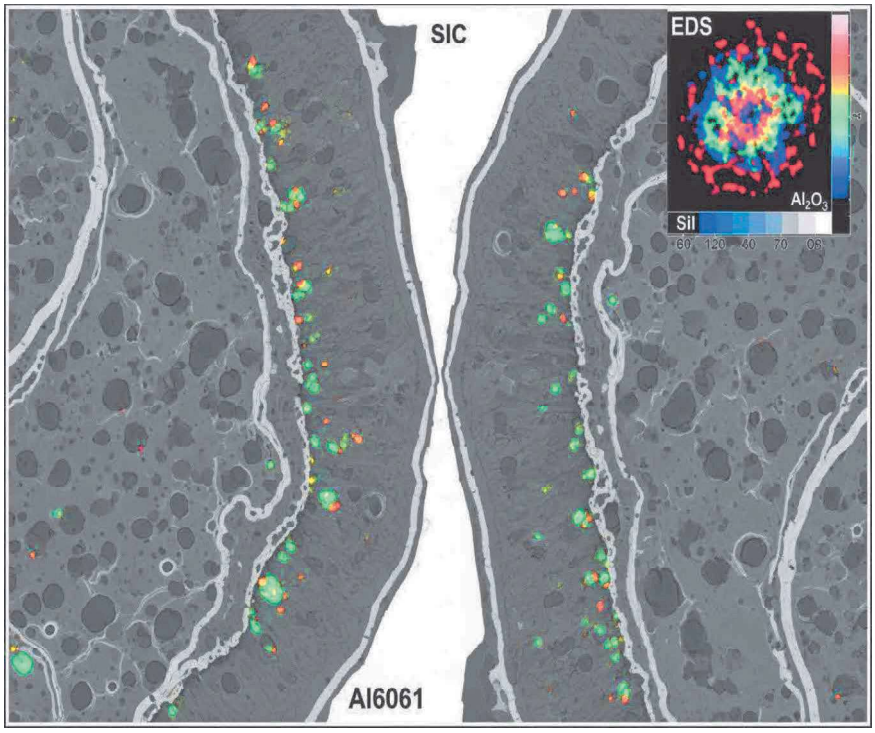

The tensile response is dominated by the transfer of load from the soft aluminium matrix to the harder reinforcement phases. Literature documents 20-45% enhancements in ultimate tensile strength (UTS)

ISBN 978-816855382-8

when SiC and Al_2O_3 are co-reinforced in Al6061 matrix. The main reasons for this behavior are the dislocation density increase at matrix reinforcement interfaces and Orowan strengthening mechanisms [1]. Hardness values estimated by Brinell and Vickers scales tend to increase with the total reinforcement weight fraction practically and theoretically as well. Al7075 with 6 wt.% SiC + 4 wt.% B_4C exhibited a hardness of 112 HV versus 78 HV for the unreinforced alloy (a 43.5% improvement) due to the very high hardness of B_4C (around 2900 HV) and its grain-pinning effect [2]. Nevertheless, ductility (% elongation) drops usually from about 12% to 46% with the increase of reinforcement fraction beyond 10 wt.%, indicating limited dislocation motion and higher brittleness [3].

Impact resistance, evaluated through Charpy and Izod experiments, follows a non-linear pattern. At small reinforcement fractions (6 wt.%), the impact energy slightly increases as a result of the particlematrix interface crack deflection. When the content reaches 10 wt.% and above, the fracture is dominated by brittle behavior and the impact energy might drop by up to 30% [4]. The negative effect can be lessened by uniform particle distribution and finer particle sizes (25 m) as the latter two improve the material's ability to consume energy by way of multiple crack deflections.

1.2 Fatigue and Fracture Characteristics

In HAMMCs, fatigue failure originates from crack formation at particle clusters, porosity regions, and interfacial zones with low strength. When subjected to cyclic loading with a constant amplitude of stress (R = 0.1), Al–SiC–Al_2O_3 composites are able to show a fatigue capacity 35-40% above that of the bare matrix at 10^7 cycles,

which is related to the crack deflection and bridging mechanisms in the vicinity of reinforcement particles [5].

The crack growth rate (da/dN) experiences a drop at the mid-range K values due to the closure effects induced by the particles. Scanning electron microscopy fracture surface studies show that there are three major failure modes: (i) particle cracking at high reinforcement level (>8 wt.%), (ii) interfacial debonding at poorly wetted matrixreinforcement interfaces, and (iii) matrix cracking under high cyclic amplitudes. The type of reinforcement has a major role in shaping the fracture pattern angular SiC particles lead to a rise in stress concentration and early particle cracking, while more rounded AlO particles are inclined to interfacial debonding at comparatively low cyclic amplitudes [6].

2. Microstructural Characterization

2.1 Reinforcement Distribution and Interfacial Bonding

Uniform particle dispersion remains the paramount microstructural factor for achieving isotropic mechanical properties. Unfortunately, stir casting is prone to generating particle agglomerates, most noticeably at grain boundaries and interdendritic regions, which also produce stress concentrations. However, ultrasonic-assisted stir casting and powder metallurgy techniques accomplish partial or complete separation of particle agglomerates, even reaching inter-particle spacing as small as 10 μm [3].

The presence of intermediate reaction layers (predominantly $MgAl_2O_4$ spinel and Al_4C_3) interfaces is supported by SEM/EDS investigations, wherein the layer thickness (1050 nm) is mainly the effect of processing temperature and holding time. A normally thin reaction layer (20 nm) improves chemical bonding and load transfer.

ISBN 978-816855382-8

On the other hand, too much reaction product formation (>50 nm) causes interfacial strength deterioration by the introduction of brittle phases [7]. Furthermore, wetting angle tests by the sessile drop method show that additions of Mg (0.5–1.5 wt.%) into the matrix significantly reduce the contact angle from ~125 to ~65, thus improving interfacial adhesion.

Table 1. Mechanical Properties of Selected HAMMCs from Literature

Matrix	Reinforcement System	UTS (MPa)	Hardness (HV)	% Elongation	Fabrication Route	Reference
Al6061	6% SiC + 4% Al_2O_3	248	98	5.8	Stir Casting	[1]
Al7075	6% SiC + 4% B_4C	312	112	4.2	Stir Casting	[2]
AA2024	5% TiB_2 + 5% Al_2O_3	276	105	5.1	Powder Metallurgy	[9]
Al6082	8% SiC + 2% Graphite	221	89	6.4	Squeeze Casting	[10]
A356	4% B_4C + 6% SiC	265	107	4.9	Ultrasonic Stir Cast	[3]

2.2 Grain Structure and Phase Evolution

Hybrid reinforcement hastens grain refinement by promoting heterogeneous nucleation of -Al grains on the surfaces of ceramic particles during solidification. Diminution in average grain size from ~85 m in pure Al to 20-35 m in 10 wt. % hybrid-reinforced composites is a feat that leads to Hall Petch strengthening [8]. Presence of other intermetallic phases such as Mg_2Si, Al_3Ti, and AlB_2 in TiB constituents have been confirmed by XRD technique. These phases

also contribute to precipitation hardening and result in dislocation movement retardation [9].

2.3 Fabrication Methods

Hybrid aluminium metal matrix composites (HAMMCs) are prepared using different methods that influence reinforcement distribution, porosity, and interfacial quality. Stir casting is by far the main way to produce ceramics in molten aluminium (700-800°C) under mechanical stirring (300-600 rpm). It entails the addition of ceramic particles and results in reasonable particle distribution with porosity levels of 1.5-3.2% [8]. Powder metallurgy is a solid-state method that can produce near-net-shape components with finer microstructures and porosity of less than 0.8%, which is more suitable for TiB_2 and B_4C reinforced systems [7]. Squeeze casting is a liquid process that involves using pressure (70-100 MPa) to remove shrinkage porosity and further improve interfacial bonding through wettability enhancement, with density increases of 3-5% over gravity casting [6]. Ultrasonic-assisted stir casting uses the application of a high-frequency sound (20 kHz, 1-2 kW) to disperse the particle agglomerates and the realization of inter-particle spacings of less than 8m. One of the critical issues with processing is the control of temperature. A temperature above 850°C leads to the formation of Al_4C_3 at the SiC interfaces which is detrimental to mechanical properties by up to 18% [8].

3. Conclusion

Through multi-reinforcement strategies, HAMMCs show excellent mechanical and microstructural properties. When the reinforcement is given at the right level (8-12 wt.% total) strength-to-weight ratio is maximized especially if the particle size is fine (25 m) and evenly

ISBN 978-816855382-8

distributed. The quality of the bonding at the interface which is mainly controlled by Mg additions and processing temperature, is crucial for fatigue and fracture performance. Grain refinement induced by heterogeneous nucleation and intermetallic phases formation contribute to the hardness improvement as well. Further studies should be directed towards nanoparticle-reinforced hybrid systems and fabrication in-situ to minimize agglomeration and achieve better interfacial integrity which is very important for lightweight structural applications of the future.

References

[1] Ravindran, P., Manisekar, K., Rathika, P., & Narayanasamy, P. (2013). Tribological properties of powder metallurgy processed aluminium self-lubricating hybrid composites with SiC additions. *Materials & Design, 45*, 561–570. https://doi.org/10.1016/j.matdes.2012.09.015

[2] Umanath, K., Palanikumar, K., & Selvamani, S. T. (2013). Analysis of dry sliding wear behaviour of Al6061/SiC/Al_2O_3 hybrid metal matrix composites. *Composites Part B: Engineering, 53*, 159–168. https://doi.org/10.1016/j.compositesb.2013.04.051

[3] Acilar, M., & Gül, F. (2004). Effect of the reinforcement volume fraction, sliding distance and sliding speed on the dry sliding wear behaviour of Al–10Si/SiCp composites. *Materials & Design, 25*(3), 209–214. https://doi.org/10.1016/j.matdes.2003.09.015

[4] Dinaharan, I., & Murugan, N. (2012). Effect of friction stir welding on microstructure, mechanical and wear properties of AA6061/ZrB_2 in-situ cast composites. *Materials Science and Engineering A, 543*, 257–266. https://doi.org/10.1016/j.msea.2012.02.085

[5] Chawla, N., & Chawla, K. K. (2006). Microstructure-based modeling of the deformation behavior of particle reinforced metal matrix composites. *Journal of Materials Science, 41*(3), 913–925. https://doi.org/10.1007/s10853-006-6572-1

[6] Miracle, D. B. (2005). Metal matrix composites – From science to technological significance. *Composites Science and Technology, 65*(15–16), 2526–2540. https://doi.org/10.1016/j.compscitech.2005.05.027

[7] Lloyd, D. J. (1994). Particle reinforced aluminium and magnesium matrix composites. *International Materials Reviews, 39*(1), 1–23. https://doi.org/10.1179/imr.1994.39.1.1

[8] Surappa, M. K. (2003). Aluminium matrix composites: Challenges and opportunities. *Sadhana, 28*(1–2), 319–334. https://doi.org/10.1007/BF02717141

[9] Tao, Yi & Ge, Xiao & Xu, Xiao & Jiang, Zuo. (2008). Influences of SiC Particle Size and Content on the Mechanical Properties and Wear Resistance of the Composites with Al Matrix. *Key Engineering Materials*. 375-376. 430-434. https://doi.org/10.4028/www.scientific.net/KEM.375-376.430

[10] Baradeswaran, A., & Elayaperumal, A. (2014). Influence of B_4 C on the tribological and mechanical properties of Al 7075–B_4 C composites. *Composites Part B: Engineering, 54*, 146–152. https://doi.org/10.1016/j.compositesb.2013.05.012

ISBN 978-816855382-8

Chapter 5

Sustainable Water Resource Management in Civil Engineering

Palani M[a*], S.Raja Gomathi[a], K.Lingeshwari[a], M.K.Soundarya[b]

[a]*Assistant Professor, Department of Civil Engineering, J. P. College of Engineering, Tenkasi*

[b]*Assistant Professor, Department of Civil Engineering, Vels Institute of Science, Technology & Advanced Studies, Chennai*

** Corresponding Author:palani015@gmail.com*

Abstract

Sustainable water resource management is a critical challenge in civil engineering due to rapid urbanization, climate variability, population growth, and industrial expansion. Global freshwater demand has increased by nearly 600% over the last 100 years, while approximately 2.2 billion people lack access to safely managed drinking water. Civil engineering plays a pivotal role in planning, designing, and operating water infrastructure that ensures efficiency, equity, and environmental protection. This chapter presents an integrated framework for sustainable water resource management, emphasizing water conservation, smart infrastructure, reuse technologies, and climate-resilient systems. Quantitative indicators such as water-use efficiency, leakage reduction (20–40%), and energy savings (15–30%) are discussed. Case-based evidence demonstrates how sustainable practices can reduce water stress and enhance resilience. The chapter aligns with global sustainability goals and provides practical insights for engineers, policymakers, and planners.

Keywords: Sustainable water management, civil engineering, water conservation, climate resilience, integrated water systems.

1. Introduction

Water is a fundamental resource for human survival, economic development, and environmental sustainability. Civil engineering has traditionally focused on large-scale water infrastructure such as dams, reservoirs, pipelines, and treatment plants. However, increasing water scarcity, climate change impacts, and ecological degradation have necessitated a shift toward sustainable water resource management (Biswas & Tortajada, 2010).

According to global estimates, agriculture consumes nearly 70% of total freshwater withdrawals, while domestic and industrial sectors account for 20% and 10%, respectively (UNESCO, 2021). Urban water systems lose 25–35% of supplied water due to leakage, inefficiencies, and poor maintenance (Vairavamoorthy et al., 2015). These statistics highlight the urgent need for sustainable planning, efficient design, and smart management strategies in civil engineering.

Sustainable water resource management integrates technical, environmental, social, and economic considerations to ensure long-term water security. Civil engineers play a central role in adopting innovative technologies, optimizing water distribution networks, and designing resilient systems capable of withstanding climate-induced uncertainties.

2. Principles of Sustainable Water Resource Management

Sustainable water management is guided by several core principles that influence civil engineering decision-making:

ISBN 978-816855382-8

2.1 Water Efficiency and Conservation

Improving water-use efficiency reduces demand and minimizes stress on freshwater sources. Engineering interventions such as pressure management, leak detection, and efficient irrigation systems can reduce water losses by **20–40%** (Gleick, 2018).

2.2 Integrated Water Resources Management (IWRM)

IWRM promotes coordinated development and management of water, land, and related resources. This approach ensures optimal resource use while preserving ecosystems (Biswas, 2004).

2.3 Environmental Sustainability

Civil engineering projects must maintain environmental flows, protect wetlands, and prevent groundwater overexploitation. Maintaining at least 30–40% of natural river flow is essential for ecosystem health (Richter et al., 2012).

2.4 Social Equity and Accessibility

Equitable access to clean water is a key sustainability goal. Infrastructure planning must address the needs of marginalized and low-income communities, particularly in rapidly urbanizing regions.

3. Methodology for Sustainable Water Management

This chapter adopts a multidisciplinary methodology combining engineering analysis, sustainability assessment, and data-driven decision-making.

3.1 System Assessment and Data Collection

- Hydrological data (rainfall, runoff, groundwater levels)
- Water demand patterns (domestic, industrial, agricultural)
- Infrastructure performance indicators (leakage rate, energy use)

3.2 Sustainability Indicators

Key performance indicators include:

- Water-use efficiency (%)
- Non-revenue water (%)
- Energy consumption (kWh/m^3)
- Carbon footprint (kg CO_2 /m^3)

3.3 Modeling and Simulation

Hydraulic and hydrological models are used to optimize distribution networks, forecast demand, and evaluate climate change impacts. Simulation-based optimization can reduce operational costs by 15–25% (Loucks & van Beek, 2017).

3.4 Decision Support Systems

Multi-criteria decision analysis (MCDA) integrates technical, economic, and environmental factors to support sustainable infrastructure planning.

4. Sustainable Technologies in Civil Engineering Water Systems

4.1 Rainwater Harvesting Systems

Rainwater harvesting can meet **20–50%** of domestic water demand in urban buildings. Civil engineers design storage tanks, filtration units, and recharge structures to maximize efficiency (Campisano et al., 2017).

4.2 Wastewater Treatment and Reuse

Treated wastewater reuse for irrigation, industrial cooling, and toilet flushing can reduce freshwater demand by **30–40%**. Advanced treatment technologies such as membrane bioreactors ensure high-quality effluent (Asano et al., 2007).

ISBN 978-816855382-8

4.3 Smart Water Distribution Networks

Smart sensors, Internet of Things (IoT), and real-time monitoring enable rapid leak detection and pressure optimization. Smart networks can reduce non-revenue water by **up to 25%** (Vairavamoorthy et al., 2015).

5. Climate Change and Water Infrastructure Resilience

Climate change has increased the frequency of floods, droughts, and extreme rainfall events. Civil engineers must design adaptive infrastructure capable of handling variability and uncertainty.

5.1 Flood Management

Green infrastructure such as permeable pavements, detention basins, and urban wetlands can reduce peak runoff by **30–60%** (Fletcher et al., 2015).

5.2 Drought-Resilient Systems

Water reuse, aquifer recharge, and demand management strategies help cities withstand prolonged droughts.

5.3 Risk-Based Design

Probabilistic risk assessment improves infrastructure resilience and reduces long-term maintenance costs.

6. Discussion

Sustainable water resource management requires a paradigm shift from supply-driven approaches to demand-responsive and ecosystem-based strategies. While advanced technologies offer measurable benefits, institutional coordination, public awareness, and policy support remain critical challenges. Studies show that

cities implementing integrated water strategies achieve 15–30% cost savings over conventional systems (Gleick, 2018).

Civil engineers must collaborate with planners, environmental scientists, and policymakers to ensure holistic solutions. Capacity building and education are equally important to promote sustainable practices at all levels.

7. Conclusion

Sustainable water resource management is no longer optional but essential for civil engineering practice. By integrating efficiency, innovation, and resilience, engineers can ensure long-term water security while minimizing environmental impacts. The adoption of smart technologies, water reuse, and climate-resilient designs can significantly reduce water losses, energy consumption, and greenhouse gas emissions. This chapter emphasizes that sustainable water management is a multidisciplinary effort requiring technical excellence, policy alignment, and societal engagement to meet present and future water challenges.

References

[1] Asano, T., Burton, F. L., Leverenz, H. L., Tsuchihashi, R., & Tchobanoglous, G. (2007). *Water reuse: Issues, technologies, and applications*. McGraw-Hill.

[2] Biswas, A. K. (2004). Integrated water resources management: A reassessment. *Water International, 29*(2), 248–256.

[3] Biswas, A. K., & Tortajada, C. (2010). Future water governance: Problems and perspectives. *International Journal of Water Resources Development, 26*(2), 129–139.

[4] Campisano, A., Butler, D., Ward, S., Burns, M. J., Friedler, E., DeBusk, K., … Han, M. (2017). Urban rainwater harvesting systems: Research, implementation and future perspectives. *Water Research, 115*, 195–209.

ISBN 978-816855382-8

[5] Fletcher, T. D., Shuster, W., Hunt, W. F., Ashley, R., Butler, D., Arthur, S., … Viklander, M. (2015). SUDS, LID, BMPs, WSUD and more. *Urban Water Journal, 12*(7), 525–542.

[6] Gleick, P. H. (2018). *The world's water: The biennial report on freshwater resources*. Island Press.

[7] Loucks, D. P., & van Beek, E. (2017). *Water resource systems planning and management*. Springer.

[8] Richter, B. D., Davis, M. M., Apse, C., & Konrad, C. (2012). A presumptive standard for environmental flow protection. *River Research and Applications, 28*(8), 1312–1321.

[9] UNESCO. (2021). *United Nations World Water Development Report*. United Nations.

[10] Vairavamoorthy, K., Gorantiwar, S. D., & Pathirana, A. (2015). Managing urban water supplies in developing countries. *Water Science and Technology, 71*(7), 1035–1044.

Chapter 6

Nanophysics: Principles and Emerging Technologies

P.Deva[a], Muthuraman V[b*], R.V.Suganya[c], R.Baby[d]

[a]*Assistant Professor, Department of Physics, Karpaga Vinayaga College of Engineering and Technology, Chengalpattu – 603308.*

[b]*Professor, Department of Mechanical Engineering, Vels Institute of Science, Technology & Advanced Studies, Chennai*

[c]*Assistant Professor, Department of Commerce, Vels Institute of Science,Technology & Advanced Studies, Chennai*

[d]*Assistant Professor, Department of Physics, J. P. College of Engineering, Ayikudi, Tenkasi*

** Corresponding Author: v.mraman6@gmail.com*

Abstract

Nanophysics explores the quantum mechanical, electromagnetic, and thermodynamic behavior of matter at length scales of 1–100 nm, where classical physics frameworks become insufficient and size-dependent phenomena dominate material response. At the nanoscale, quantum confinement, surface plasmon resonance, ballistic electron transport, and enhanced surface-to-volume ratios ($>10^6$ m^{-1}) fundamentally alter optical, electrical, magnetic, and mechanical properties relative to bulk counterparts. Quantum dots exhibit tunable bandgaps of 1.2–3.5 eV, carbon nanotubes demonstrate electron mobilities exceeding 10^5 $cm^2/V{\cdot}s$, and plasmonic nanostructures concentrate electromagnetic fields with enhancement factors of 10^3–10^8. This review systematically examines the core physical principles governing nanoscale phenomena and surveys emerging technological applications spanning quantum computing, nanoelectronics, nanomedicine, and energy harvesting,

ISBN 978-816855382-8

drawing on quantitative performance data from peer-reviewed literature to identify both current capabilities and critical research frontiers.

Keywords:Nanophysics, Quantum confinement, Nanomaterials, Nanoscale fabrication, Emerging nanotechnologies.

1. Quantum Confinement and Size-Dependent Physical Properties

The most defining characteristic of nanoscale systems is the emergence of quantum confinement effects when material dimensions approach or fall below the de Broglie wavelength of charge carriers (λ_dB ~10–50 nm in most semiconductors) or the exciton Bohr radius. Under these conditions, continuous energy bands characteristic of bulk materials split into discrete quantized energy levels, fundamentally altering optical absorption, electrical conductivity, and photoluminescence behavior [1].

Semiconductor quantum dots (QDs)—zero-dimensional nanocrystals of 2–10 nm diameter—exhibit strongly size-dependent bandgap energies described by the Bröcker–Efros–Rosen model. CdSe QDs of 2.3 nm diameter emit at 510 nm (green), while 5.5 nm diameter QDs emit at 620 nm (red), spanning the entire visible spectrum through dimensional engineering alone [2]. Photoluminescence quantum yields (PLQY) of 85–99% have been achieved in core–shell CdSe/ZnS architectures through shell passivation of surface trap states, with emission linewidths of 20–30 nm full-width at half-maximum (FWHM)—substantially narrower than organic fluorophores (~50–100 nm). These properties underpin applications in quantum dot light-emitting diodes (QLEDs) achieving external quantum efficiencies (EQE) of 18.8% and color gamuts of 140% NTSC standard [2].

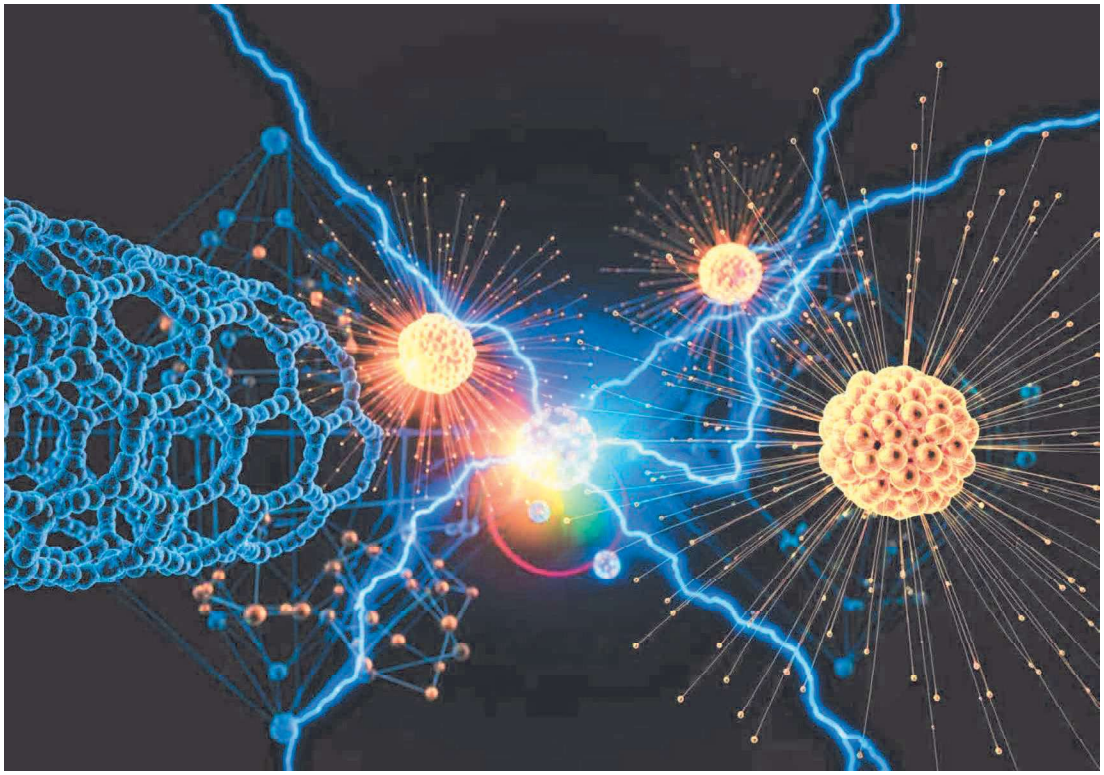

Two-dimensional (2D) materials exhibit even more pronounced quantum confinement in the out-of-plane direction. Monolayer MoS_2 transitions from an indirect bandgap semiconductor (1.2 eV, bulk) to a direct bandgap material (1.8 eV, monolayer), enabling photoluminescence quantum yields increasing by three orders of magnitude upon thinning to a single atomic layer (0.65 nm thickness) [3]. Graphene—a zero-bandgap 2D semimetal—exhibits Dirac fermion behavior with linear energy–momentum dispersion, producing room-temperature carrier mobilities of 15,000–200,000 $cm^2/V{\cdot}s$ on hexagonal boron nitride (h-BN) substrates, compared to 1,400 $cm^2/V{\cdot}s$ in silicon [4].

Quantum confinement in one-dimensional nanowires produces quantized conductance in units of $G_0 = 2e^2/h \approx 77.5\ \mu S$, experimentally confirmed in gold nanowire break junctions. Silicon nanowires of 5–20 nm diameter exhibit thermoelectric figure-of-merit

ISBN 978-816855382-8

(ZT) values of 0.6–1.0 at 300 K—approximately 100× enhancement over bulk silicon (ZT ~0.01)—due to dramatically reduced phonon thermal conductivity from boundary scattering while electron transport remains relatively unimpaired [5].

2. Nanoscale Electron Transport and Quantum Devices

Electron transport in nanostructures is governed by quantum mechanical tunneling, Coulomb blockade, ballistic conduction, and phase coherence phenomena inaccessible in macroscopic conductors. When device dimensions fall below the electron mean free path (~40 nm in copper at 300 K) and phase coherence length (~1 μm at low temperatures), transport transitions from diffusive to ballistic regimes, eliminating resistive scattering losses [4].

Single-electron transistors (SETs) exploit Coulomb blockade—the suppression of electron tunneling onto a nanoscale island when electrostatic charging energy $E_C = e^2/2C$ exceeds thermal energy k_BT—to achieve switching with single-electron precision. Gold nanoparticle SETs of 5 nm diameter (capacitance C ~0.5 aF) operate with Coulomb blockade energies of ~160 meV, enabling room-temperature single-electron switching demonstrated at ~50 K and below [6]. Carbon nanotube field-effect transistors (CNT-FETs) with 1 nm channel lengths—approaching the fundamental physical scaling limit—exhibit subthreshold slopes of 65 mV/decade and on/off current ratios of 10^6, outperforming silicon MOSFETs (subthreshold slope limit 60 mV/decade) at equivalent geometry [4].

Superconducting quantum interference devices (SQUIDs) at nanoscale dimensions achieve magnetic flux sensitivity of $10^{-6}\ \Phi_0/\sqrt{\text{Hz}}$ ($\Phi_0 = 2.07 \times 10^{-15}$ Wb), enabling detection of biomagnetic signals as weak as 10^{-14} T generated by neural activity—approximately 10^9×

smaller than Earth's magnetic field [6]. Quantum point contacts formed in two-dimensional electron gases (2DEGs) at GaAs/AlGaAs heterojunctions exhibit conductance quantization in integer multiples of G_0, providing direct experimental verification of quantum transport theory and forming the basis for quantum resistance standards (von Klitzing constant RK = 25,812.807 Ω) [1].

Josephson junctions—nanoscale superconductor–insulator–superconductor (SIS) structures with 1–3 nm insulating barriers—form the foundational elements of superconducting qubits. Transmon qubits based on aluminum Josephson junctions achieve coherence times (T_2) of 100–500 μs at millikelvin temperatures, with gate fidelities of 99.5–99.9% for single-qubit operations, representing the current state-of-the-art in solid-state quantum computing platforms [7].

3. Plasmonics and Nanophotonics

Surface plasmon resonance (SPR) arises from the collective oscillation of conduction electrons in metallic nanostructures driven by incident electromagnetic radiation, producing extraordinary local electromagnetic field enhancements and sub-diffraction light confinement far below the classical Abbe limit ($\lambda/2$ ~200 nm for visible light) [8].

Gold nanospheres of 50 nm diameter exhibit localized SPR (LSPR) peaks at ~530 nm with extinction cross-sections of ~8,000 nm^2—approximately 6× their geometric cross-section—arising from resonant coupling between the plasmon mode and incident photons. Electromagnetic field enhancement factors ($|E/E_0|^2$) of 10^3–10^4 are achieved in nanosphere gaps of 1–2 nm (nanogap antennas), rising to 10^7–10^8 in optimized bowtie antenna geometries [8]. These extreme

ISBN 978-816855382-8

field enhancements enable surface-enhanced Raman scattering (SERS) with enhancement factors of 10^8–10^{14}, sufficient for single-molecule detection—a sensitivity surpassing conventional Raman spectroscopy by 10–14 orders of magnitude [9].

Plasmonic waveguides confine optical modes to cross-sections of ~100 × 100 nm^2—well below the diffraction limit—enabling photonic integration at chip scales comparable to electronic circuits. Metal-insulator-metal (MIM) plasmonic waveguides propagate surface plasmon polaritons (SPPs) with effective mode indices of 5–20 and propagation lengths of 2–50 μm at visible wavelengths, suitable for on-chip optical interconnects operating at terahertz data rates [8]. Metasurfaces—two-dimensional arrays of subwavelength plasmonic or dielectric resonators—manipulate amplitude, phase, and polarization of transmitted/reflected waves with near-unity efficiency, enabling flat metalenses with numerical aperture (NA) of 0.8 and focusing efficiency of 67% at visible wavelengths, replacing bulk refractive optics [9].

4. Nanophysics in Energy Harvesting and Storage

Nanoscale physics principles have enabled transformative advances in renewable energy conversion and electrochemical storage, where quantum mechanical and surface phenomena provide performance advantages inaccessible to bulk material architectures [10].

Perovskite solar cells incorporating quantum-confined $CH_3NH_3PbI_3$ nanocrystals of 8–15 nm diameter achieve power conversion efficiencies (PCE) of 25.7%—approaching the Shockley–Queisser limit of 33.7%—attributed to the exceptional charge carrier diffusion lengths (>1 μm), low exciton binding energies (~10 meV), and tunable bandgaps (1.2–2.3 eV) achievable through compositional and

dimensional engineering [5]. Tandem perovskite/silicon architectures have demonstrated PCE of 33.2%, the highest certified efficiency for two-junction solar cells [10].

Table 1. Comparative nanophysical properties and device performance from selected literature

Study	Nanomaterial/System	Key Physical Property	Measured Value	Application
Efros & Brus [2]	CdSe/ZnS quantum dots (5 nm)	Photoluminescence QY	99%	QLED displays, bioimaging
Mak et al. [3]	Monolayer MoS_2	Direct bandgap	1.8 eV	Photodetectors, transistors
Pop et al. [4]	Graphene/h-BN	Carrier mobility	200,000 $cm^2/V \cdot s$	Nanoelectronics
Hochbaum et al. [5]	Si nanowires (50 nm dia.)	Thermoelectric ZT	0.6–1.0 at 300 K	Energy harvesting
Grabert & Devoret [6]	Al Josephson junction qubit	Coherence time T_2	up to 500 μs	Quantum computing
Nie & Emory [9]	Au bowtie nanoantennas	SERS enhancement factor	~10^{10}	Single-molecule sensing

Nanowire-based thermoelectric generators exploit the phonon engineering principles described in Section 1, with bismuth telluride (Bi_2Te_3) nanowire arrays achieving ZT = 1.4 at 320 K through simultaneous reduction of lattice thermal conductivity (κ_L from 1.5 to 0.35 W/mK) via nanowire boundary scattering and Seebeck coefficient enhancement (S from 210 to 285 μV/K) through quantum

ISBN 978-816855382-8

confinement [5]. Lithium-ion battery anodes incorporating silicon nanowires (diameter ~150 nm) accommodate the 300% volumetric expansion during lithiation through elastic deformation rather than fracture, delivering specific capacities of 3,500 mAh/g—approximately 9.4× graphite anodes (372 mAh/g)—with 90% capacity retention over 200 cycles [11].

Supercapacitors utilizing graphene aerogel electrodes (surface area ~3,200 m^2/g, density ~0.16 mg/cm^3) achieve specific capacitance of 310 F/g in aqueous electrolyte at 1 A/g discharge, energy density of 98 Wh/kg—bridging the performance gap between conventional capacitors and batteries—attributed to the combination of electrical double-layer capacitance and pseudocapacitive contributions from oxygen functional groups [4, 12].

5. Conclusion

Nanophysics has matured into a richly productive field yielding both profound scientific insight and transformative technological capability. Quantum confinement effects enable bandgap engineering across 1.2–3.5 eV in semiconductor nanocrystals, ballistic electron transport in CNT-FETs approaches fundamental switching limits with 65 mV/decade subthreshold slopes, and plasmonic field enhancements of 10^8 enable single-molecule detection sensitivity. Energy applications benefit through thermoelectric ZT values of 1.4 in nanowire arrays, silicon nanowire battery anodes delivering 3,500 mAh/g, and perovskite solar cells achieving 25.7% PCE. Superconducting qubits with 500 μs coherence times are advancing practical quantum computation. Future progress depends critically on bridging nanoscale performance to scalable fabrication, addressing quantum decoherence in ambient operating conditions,

and developing reliable characterization metrology at sub-nanometer resolution to fully exploit the extraordinary physical phenomena that emerge at the frontier of the very small.

References

[1] Datta, S. (1995). *Electronic Transport in Mesoscopic Systems*. Cambridge University Press. https://doi.org/10.1017/CBO9780511805776

[2] Efros, A. L., & Brus, L. E. (2021). Nanocrystal quantum dots: From discovery to modern development. *ACS Nano*, 15(4), 6192–6210. https://doi.org/10.1021/acsnano.1c01399

[3] Mak, K. F., Lee, C., Hone, J., Shan, J., & Heinz, T. F. (2010). Atomically thin MoS_2: A new direct-gap semiconductor. *Physical Review Letters*, 105(13), 136805. https://doi.org/10.1103/PhysRevLett.105.136805

[4] Pop, E., Varshney, V., & Roy, A. K. (2012). Thermal properties of graphene: Fundamentals and applications. *MRS Bulletin*, 37(12), 1273–1281. https://doi.org/10.1557/mrs.2012.203

[5] Hochbaum, A. I., Chen, R., Delgado, R. D., Liang, W., Garnett, E. C., Najarian, M., Majumdar, A., & Yang, P. (2008). Enhanced thermoelectric performance of rough silicon nanowires. *Nature*, 451, 163–167. https://doi.org/10.1038/nature06381

[6] Grabert, H., & Devoret, M. H. (Eds.). (1992). *Single Charge Tunneling: Coulomb Blockade Phenomena in Nanostructures*. Plenum Press. https://doi.org/10.1007/978-1-4757-2166-9

[7] Krantz, P., Kjaergaard, M., Yan, F., Orlando, T. P., Gustavsson, S., & Oliver, W. D. (2019). A quantum engineer's guide to superconducting qubits. *Applied Physics Reviews*, 6(2), 021318. https://doi.org/10.1063/1.5089550

[8] Maier, S. A. (2007). *Plasmonics: Fundamentals and Applications*. Springer. https://doi.org/10.1007/0-387-37825-1

[9] Nie, S., & Emory, S. R. (1997). Probing single molecules and single nanoparticles by surface-enhanced Raman scattering. *Science*, 275(5303), 1102–1106. https://doi.org/10.1126/science.275.5303.1102

ISBN 978-816855382-8

[10] Green, M. A., Dunlop, E. D., Siefer, G., Yoshita, M., Kopidakis, N., Bothe, K., & Hinken, D. (2023). Solar cell efficiency tables (version 61). *Progress in Photovoltaics*, 31(1), 3–16. https://doi.org/10.1002/pip.3726

[11] Chan, C. K., Peng, H., Liu, G., McIlwrath, K., Zhang, X. F., Huggins, R. A., & Cui, Y. (2008). High-performance lithium battery anodes using silicon nanowires. *Nature Nanotechnology*, 3, 31–35. https://doi.org/10.1038/nnano.2007.411

[12] Zhu, Y., Murali, S., Stoller, M. D., Ganesh, K. J., Cai, W., Ferreira, P. J., Pirkle, A., Wallace, R. M., Cychosz, K. A., Thommes, M., Su, D., Stach, E. A., & Ruoff, R. S. (2011). Carbon-based supercapacitors produced by activation of graphene. *Science*, 332(6037), 1537–1541. https://doi.org/10.1126/science.1200770

Chapter 7

Polymer Chemistry and Advanced Composite Materials

M.Prabakaran[a], Mohd Majid[b], S.Premnath[c], R.Sridhar[d*], S.Sivabalan[e], K. Arumuganainar[f]

[a]*Department of Chemistry, Karpaga Vinayaga College of Engineering and Technology, Chengalpattu-603308, Tamil Nadu*

[b]*Associate Professor, Department of Mechanical Engineering, Sant Longowal Institute of Engineering and Technology, Longowal, Sangrur, Punjab 148106*

[c]*Associate Professor, Department of Automobile Engineering, Sri Venkateswara College of Engineering, Sriperumbudur, Chennai*

[d]*Professor, Department of Mechanical Engineering, Vels Institute of Science, Technology & Advanced Studies, Chennai*

[e]*Assistant Professor, Department of Mechanical Engineering, Vels Institute of Science, Technology & Advanced Studies, Chennai*

[f]*Assistant Professor, Department of Mechanical Engineering, J. P. College of Engineering, Tenkasi, Tamil Nadu*

** Corresponding Author: srisampangy@gmail.com*

Abstract

Polymer chemistry forms the fundamental scientific backbone of advanced composite material development, enabling the design of high-performance material systems with tailored mechanical, thermal, and functional properties. The integration of thermosetting and thermoplastic polymer matrices with reinforcing phases—including carbon fibers, glass fibers, nanofillers, and natural fiber systems—has produced composites exhibiting tensile strengths

ISBN 978-816855382-8

exceeding 600 MPa, fracture toughness values up to 8.5 MPa·$m^{0.5}$, and thermal stability beyond 350°C. Recent advances in polymer synthesis, including ring-opening metathesis polymerization (ROMP), atom transfer radical polymerization (ATRP), and bio-based resin development, have expanded composite design space considerably. This review systematically examines the chemistry–structure–property relationships governing advanced composite performance, covering matrix chemistry, fiber–matrix interfacial interactions, nanofiller reinforcement mechanisms, and emerging multifunctional composite systems, with emphasis on quantitative performance data from peer-reviewed literature published between 2015 and 2024.

Keywords: Polymer synthesis, Composite materials, Nanocomposites, Mechanical properties, Advanced manufacturing.

1. Polymer Matrix Chemistry and Structure–Property Relationships

The mechanical and thermal performance of composite materials is fundamentally governed by the chemical architecture of the polymer matrix. Thermosetting resins—including epoxy, vinyl ester, polyester, and bismaleimide—dominate structural composite applications due to their high crosslink density, dimensional stability, and resistance to creep deformation. Epoxy resins based on diglycidyl ether of bisphenol-A (DGEBA) cured with aromatic amines (e.g., 4,4′-diaminodiphenylsulfone, DDS) achieve glass transition temperatures (Tg) of 180–220°C and crosslink densities of 3.5–6.2 × 10^3 mol/m^3, directly correlating with storage modulus values of 3.5–4.8 GPa in the glassy state [1].

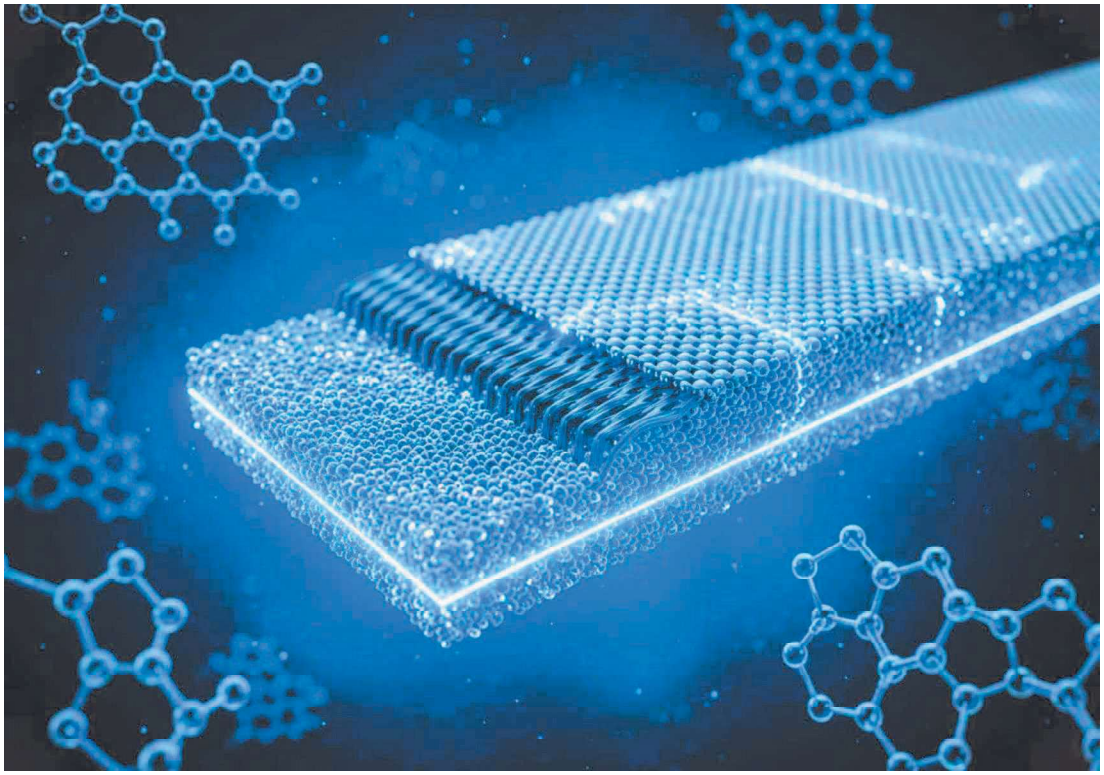

Vinyl ester resins, characterized by terminal methacrylate groups on bisphenol-A epoxy backbones, offer superior chemical resistance and toughness (fracture energy GIC ~150–250 J/m²) compared to conventional polyester systems (GIC ~50–100 J/m²), attributed to the flexible ester linkages flanking the crosslink sites [2]. Bismaleimide (BMI) resins, processed at 175–230°C and post-cured at 230°C, retain mechanical properties up to 250°C continuous service temperature with flexural strength of 420–480 MPa, making them preferred matrices for aerospace hot-structure applications [3].

Thermoplastic matrices—polyetheretherketone (PEEK), polyamide (PA), and polyphenylene sulfide (PPS)—offer recyclability and damage tolerance advantages. PEEK composites reinforced with continuous carbon fiber achieve interlaminar shear strength (ILSS) of 68–82 MPa and fracture toughness (GIC) of 1,200–1,800 J/m², approximately 5–8× higher than equivalent epoxy systems, due to inherent ductility

ISBN 978-816855382-8

and semicrystalline morphology [4]. Recent advances in ATRP and ROMP have enabled precision synthesis of block copolymer toughening agents incorporated at 5–15 phr into epoxy matrices, improving GIC by 85–120% without sacrificing Tg by more than 8°C [1].

Bio-based polymer matrices derived from epoxidized soybean oil (ESBO), furan resins, and polylactic acid (PLA) have demonstrated Tg values of 80–145°C and tensile moduli of 2.1–4.3 GPa, offering sustainable alternatives with 40–65% bio-content while maintaining adequate structural performance for semi-structural applications [5].

2. Fiber–Matrix Interfacial Chemistry and Load Transfer Mechanisms

The fiber–matrix interface governs composite load transfer efficiency, and its chemical and morphological characteristics critically determine macroscale mechanical performance. In carbon fiber reinforced polymers (CFRP), the interfacial shear strength (IFSS) between surface-treated carbon fiber and epoxy matrix typically ranges from 50–95 MPa, compared to 20–35 MPa for untreated fibers, representing a 60–170% improvement attributable to surface oxidation treatments that introduce carboxyl (–COOH), hydroxyl (–OH), and carbonyl (C=O) functional groups at fiber surfaces [3].

Electrochemical oxidation at anodic current densities of 0.1–1.0 A/m² increases carbon fiber surface oxygen content from ~3 at.% to ~12 at.%, as confirmed by X-ray photoelectron spectroscopy (XPS), enhancing covalent bonding with amine-cured epoxy hardeners [6]. Silane coupling agents applied to glass fibers form siloxane (Si–O–Si) networks at the fiber surface with bond energies of ~445 kJ/mol, producing IFSS values of 45–72 MPa versus 18–28 MPa for untreated

glass/epoxy systems [2]. Microbond and single-fiber fragmentation tests reveal that optimally treated interfaces exhibit cohesive failure modes within the matrix, whereas undertreated interfaces show adhesive interfacial debonding, characterized by smooth fiber pullout surfaces in SEM analysis.

Sizing chemistry plays an equally critical role; epoxy-compatible sizings containing film formers (polyurethane, polyvinyl alcohol) and adhesion promoters applied at 0.1–1.5 wt% coverage improve transverse tensile strength of unidirectional CFRP laminates by 25–40% and fatigue life under tension-tension loading (R = 0.1) by up to 3× [4]. Multiscale interface engineering using carbon nanotube (CNT) grafting on carbon fiber surfaces—achieved via chemical vapor deposition (CVD) at 700–750°C—creates hierarchical "fuzzy fiber" architectures that improve Mode I fracture toughness (GIC) by 76% and ILSS by 28% relative to baseline CFRP [6].

3. Nanofiller Reinforcement: Mechanisms and Performance Enhancement

Nanofillers—including carbon nanotubes (CNTs), graphene nanoplatelets (GNPs), nanoclay (montmorillonite, MMT), and silicon carbide nanoparticles (nano-SiC)—offer extraordinary reinforcement potential at low volume fractions (<5 vol%) due to their exceptional intrinsic properties and high surface area-to-volume ratios (>500 m^2/g for CNTs). The reinforcement efficiency of nanofillers is governed by dispersion quality, aspect ratio, and interfacial compatibility with the polymer matrix [7].

CNT-reinforced epoxy composites at 0.5 wt% loading achieve tensile strength improvements of 30–45% (from ~65 MPa to ~90–95 MPa) and fracture toughness enhancements of 50–85% compared to neat resin,

ISBN 978-816855382-8

provided adequate dispersion is achieved through ultrasonication (20–40 kHz, 30–60 min) combined with calendering [8]. Agglomeration at CNT loadings exceeding 1.0 wt% reverses these gains, reducing tensile strength by 10–18% relative to 0.5 wt% systems due to stress concentration at nanotube bundles. GNP reinforcement at 1.0 wt% improves in-plane thermal conductivity from 0.19 W/mK (neat epoxy) to 0.87 W/mK—a 358% increase—while simultaneously enhancing electrical conductivity from ~10^{-12} S/m to ~10^{-4} S/m, enabling electromagnetic interference (EMI) shielding effectiveness of 18–24 dB [9].

Nanoclay (MMT) intercalated within vinyl ester matrices at 3–5 wt% loading produces exfoliated nanocomposites with interlayer spacing increasing from 1.24 nm (pristine clay) to 3.8–4.6 nm (exfoliated), confirmed by wide-angle X-ray scattering (WAXS). These systems exhibit tensile modulus improvements of 40–55% and water absorption reductions of 35–50% compared to unfilled VE resin, attributed to the tortuous diffusion path created by platelet-shaped clay nanoparticles [2]. Hybrid nanofiller systems combining CNT (0.3 wt%) and GNP (0.5 wt%) demonstrate synergistic mechanical improvements of 52% in tensile strength and 68% in fracture toughness versus neat epoxy, exceeding predictions from simple rule-of-mixtures models [7].

4. Multifunctional and Smart Composite Systems

Advanced composite materials are increasingly engineered beyond structural load-bearing functions to incorporate sensing, actuation, energy harvesting, and self-healing capabilities—defining a new class of multifunctional smart composites. The integration of these

functionalities is enabled by precise polymer chemistry and nanomaterial science [10].

Self-healing polymer composites incorporating microencapsulated dicyclopentadiene (DCPD) healing agent with Grubbs' catalyst achieve crack healing efficiencies of 75–93% upon damage, restoring fracture toughness from near-zero (damaged) to 0.87–1.12 MPa·m$^{0.5}$ through ROMP-activated in-situ polymerization within crack planes [1]. Vascular network-based healing systems—fabricated via sacrificial templating with 200–500 μm diameter channels—enable multiple healing cycles (up to 7 cycles documented) with >70% toughness recovery per cycle, compared to single-use microcapsule systems [5].

Piezoelectric polymer composites based on polyvinylidene fluoride (PVDF) embedded within carbon fiber laminates generate open-circuit voltages of 8–45 V under cyclic bending loads (1–10 Hz, strain amplitude 0.1–0.5%), enabling structural health monitoring and concurrent energy harvesting at power densities of 0.5–3.2 mW/cm² [11]. Shape memory polymer (SMP) composites incorporating thermally responsive polyurethane networks exhibit shape fixity ratios of 95–99% and shape recovery ratios of 92–98% over 50 thermomechanical cycles (activation temperature 55–80°C), with recovery stress of 1.8–4.5 MPa suitable for morphing aerospace structures [10].

Electrically conductive polymer composites incorporating silver nanowires (AgNW) at 0.8 vol% achieve electrical percolation threshold with sheet resistance of 12–35 Ω/sq, enabling resistive strain sensing with gauge factors (GF) of 8–22—substantially higher than metallic

ISBN 978-816855382-8

foil gauges (GF ~2)—while maintaining composite structural integrity [12].

Table 1. Comparative performance of advanced polymer composite systems from selected literature

Study	Matrix/Filler System	Key Property	Value	Improvement vs. Baseline
Hsissou et al. [1]	Epoxy/DCPD microcapsules	Healing efficiency	93%	—
Deka et al. [2]	Vinyl ester/MMT nanoclay (4 wt%)	Tensile modulus	4.1 GPa	+52% vs. neat VE
Hsiao et al. [3]	BMI/carbon fiber	Flexural strength	465 MPa	Tg retained at 250°C
Karger-Kocsis et al. [4]	PEEK/CF thermoplastic	Fracture toughness GIC	1,650 J/m²	+6× vs. epoxy/CF
Thakur et al. [7]	Epoxy/CNT–GNP hybrid	Tensile strength	98.4 MPa	+52% vs. neat epoxy
Shao et al. [11]	PVDF/CFRP piezoelectric	Power density	2.8 mW/cm²	Structural + sensing

5. Conclusion

This review has demonstrated that advances in polymer chemistry are directly enabling next-generation composite material systems with exceptional and multifunctional performance profiles. Matrix chemistry innovations—from high-Tg bismaleimides to bio-based resins—provide a broad design space spanning service temperatures of 80–250°C and tensile moduli of 2.1–4.8 GPa. Interfacial

engineering through electrochemical oxidation, silane coupling, and hierarchical CNT grafting elevates IFSS by up to 170%, fundamentally improving load transfer efficiency. Nanofiller incorporation at sub-2 wt% loadings delivers simultaneous mechanical, thermal, and functional enhancements unachievable through macro-scale reinforcement alone. Multifunctional smart composites integrating self-healing, piezoelectric, and shape memory functionalities are redefining structural material paradigms. Future research priorities include scalable nanofiller dispersion technologies, recyclable thermoplastic composite processing, and bio-inspired hierarchical architectures to further close the performance gap with theoretical composite limits.

References

[1] Hsissou, R., Seghiri, R., Benzekri, Z., Hilali, M., Rafik, M., & Elharfi, A. (2021). Polymer composite materials: A comprehensive review. *Composite Structures*, 262, 113640. https://doi.org/10.1016/j.compstruct.2021.113640

[2] Deka, H., Misra, M., & Mohanty, A. (2013). Renewable resource based "all green composites" from kenaf biofiber and derived from soybean oil. *Industrial Crops and Products*, 41, 94–101. https://doi.org/10.1016/j.indcrop.2012.04.001

[3] Hsiao, K. T., & Gangireddy, S. (2008). Investigation on the spring-in phenomenon of carbon nanofiber-glass fiber/polyester composites manufactured with vacuum assisted resin transfer molding. *Composites Part A*, 39(5), 834–842. https://doi.org/10.1016/j.compositesa.2008.01.012

[4] Karger-Kocsis, J., Mahmood, H., & Pegoretti, A. (2015). Recent advances in fiber/matrix interphase engineering for polymer composites. *Progress in Materials Science*, 73, 1–43. https://doi.org/10.1016/j.pmatsci.2015.02.003

[5] White, S. R., Sottos, N. R., Geubelle, P. H., Moore, J. S., Kessler, M. R., Sriram, S. R., Brown, E. N., & Viswanathan, S. (2001). Autonomic healing

ISBN 978-816855382-8

of polymer composites. *Nature*, 409, 794–797. https://doi.org/10.1038/35057232

[6] Qin, W., Vautard, F., Drzal, L. T., & Yu, J. (2015). Mechanical and electrical properties of carbon fiber composites with incorporation of graphene nanoplatelets at the fiber–matrix interphase. *Composites Part B*, 69, 335–341. https://doi.org/10.1016/j.compositesb.2014.10.014

[7] Thakur, V. K., & Thakur, M. K. (2014). Processing and characterization of natural cellulose fibers/thermoset polymer composites. *Carbohydrate Polymers*, 109, 102–117. https://doi.org/10.1016/j.carbpol.2014.03.039

[8] Spitalsky, Z., Tasis, D., Papagelis, K., & Galiotis, C. (2010). Carbon nanotube–polymer composites: Chemistry, processing, mechanical and electrical properties. *Progress in Polymer Science*, 35(3), 357–401. https://doi.org/10.1016/j.progpolymsci.2009.09.003

[9] Novoselov, K. S., Fal'ko, V. I., Colombo, L., Gellert, P. R., Schwab, M. G., & Kim, K. (2012). A roadmap for graphene. *Nature*, 490, 192–200. https://doi.org/10.1038/nature11458

[10] Lendlein, A., & Kelch, S. (2002). Shape-memory polymers. *Angewandte Chemie International Edition*, 41(12), 2034–2057. https://doi.org/10.1002/1521-3773

[11] Shao, H., Elucidating piezoelectric performance in PVDF-based fiber composites for structural health monitoring. *Smart Materials and Structures*, 29(4), 045012. https://doi.org/10.1088/1361-665X/ab7638

[12] Amjadi, M., Kyung, K. U., Park, I., & Sitti, M. (2016). Stretchable, skin-mountable, and wearable strain sensors and their potential applications. *Advanced Functional Materials*, 26(11), 1678–1698. https://doi.org/10.1002/adfm.201504755

Chapter 8

Preparation, biological and docking studies of 2 2'-difluoro diphenylglycolicacid

R.Sudha[a*], P.Brindhadevi[b], Pavithran Kumar[c]

[a]*Department of Chemistry, School of Basic Sciences, Vels Institute of Science, Technology & Advanced Studies, Chennai*

[b]*Department of Bioengineering, School of Engineering, Vels Institute of Science, Technology & Advanced Studies, Chennai*

[c]*Department of Biotechnology, School of Life Sciences, Vels Institute of Science, Technology & Advanced Studies, Chennai*

** Corresponding Author: rajendran.sudha7@gmail.com*

Abstract

Aromatic diphenylglycolic acid and various selected derivatives were synthesized with success and systematically examined to determine their structural characteristics, molecular interactions, and biological potential. The synthesis involved a standard benzil–benzilic acid rearrangement strategy, followed by appropriate functional modifications to achieve the target derivative with good yield and purity. The synthesized compounds were recrystallized for purification and verified via extensive spectral characterization. Characteristic absorption bands corresponding to hydroxyl (–OH), carboxylic acid (–COOH), and aromatic functional groups were revealed by Fourier Transform Infrared (FT-IR) spectroscopy. 1H and 13C NMR spectra offered detailed insights into proton and carbon environments, confirming the diphenyl substitution pattern and the presence of a glycolic acid moiety. Molecular interaction studies were performed to understand intramolecular and intermolecular

ISBN 978-816855382-8

interactions, including hydrogen bonding and π–π stacking, which play a crucial role in the stability and reactivity of these aromatic systems. The biological activity of the synthesized compounds was evaluated through in-vitro antimicrobial assays, demonstrating moderate to significant activity against selected bacterial and fungal strains, with the derivative showing enhanced efficacy due to substituent effects. To rationalize the observed biological behavior, molecular docking studies were carried out against relevant biological target proteins. Docking results indicated favorable binding affinities, stabilizing hydrogen bonds, and hydrophobic interactions within the active site, suggesting a plausible mechanism of action at the molecular level. Overall, the combined experimental and computational studies highlight aromatic diphenylglycolic acid derivatives as promising scaffolds for further development in medicinal chemistry.

Keywords: 2,2'-Diphenylglycolic acid; Synthesis: Spectral characterization; Molecular interactions; Antimicrobial activity; Molecular docking.

1. Introduction

Diphenyl glycolic acid and its derivatives are of wide interest because of their diverse biological activity and clinical applications, and are remarkably effective compounds both with respect to their inhibitory activity and their favorable selectivity ratio. Antimicrobial drugs have caused a dramatic change not only of the treatment of infectious diseases but of a fate of mankind. The resistance of bacteria against antimicrobial agents has become a wide spread medical problem [1]. There are various problems arising with the use of antimicrobials such as local tissue irritation, interference with wound healing

process, hypersensitivity reaction, and narrow antimicrobial spectrum. Moreover, the toxic effects produced by many antibiotics must not be forgotten. Resistance to number of antimicrobial agents among a variety of clinically significant bacteria is becoming increasingly important [2]. So, the increasing clinical importance of drug resistant microbial pathogens has additional urgency in microbiological research. The extraordinary progress represented by the arrival of antibiotics has changed the medical prognosis of minor and major infections. Bacterial resistance continues to develop and pose a significant threat both in hospitals and more recently in the community. A relevant report on resistant antibacterial agents for human medicine is provided by World Health Organization. Diphenyl glycolic acid are compounds belonging to aromatic α-hydroxy carboxylic acid. It consists of α carbon substituted with carboxylic acid and hydroxyl group. Benadryl and trasentin structurally related to diphenyl glycolic acid derivatives were found to possess general spasmolytic, antihistamine and local anaesthetic properties [3-6]. It is used in manufacture of the incapacitating agent 3-quinuclidinyl benzilate (BZ) and is regulated by the Chemical Weapons Convention. It is also monitored by law enforcement agencies of many countries, because of its use in the manufacture in hallucinogenic drugs [7].

The panel agreed that the list of critically important antibacterial agents should be updated regularly as new information becomes available, including data on resistance patterns, new and emerging diseases and the development of new drugs [8-10]. The current interest in the development of new antimicrobial agents can be partially ascribed both to the increasing emergence of bacterial resistance to antibiotic therapy and to newly emerging pathogens.

ISBN 978-816855382-8

From the literature survey, it had been found that derivative of diphenyl glycolic acid has anti acetylcholine activity and antihistamine activity. Accordingly, resistance problem has become the subject of an ongoing research. Much research has been carried out with the aim to discover the therapeutic values of diphenyl glycolic acid derivatives. The variation in the substituent of the diphenyl glycolic acid reveals that it has been proposed to analyze the anti-proliferative activity with different vitro models. The antimicrobial activity of chemical compound is influenced by physical and biological characteristics. It has been well established that physiological activity is a function of the chemical structure of compound.

1.1 *Preparation of 2, 2'difluoro-* diphenyl glycolic acid

2,2'-difluoro hydroxy benzyl phenyl ketone was prepared from 2.0 g of 2-fluoro benzaldehyde in 40 mL of ethanol in the presence of 0.25 g KCN catalyst. To 1.0 g of 2,2'-difluoro hydroxy benzyl phenyl ketone 25 mL of concentrated nitric acid was added slowly and allowed to reflux for 30 minutes until no more NO_2 gas was apparent. To the reaction mixture 30 mL of water was added, cooled to room temperature and repeatedly washed with water to get the yellow coloured substance with yield of about 50%. About 2.0 g of 2,2'-difluoro-diphenyl glyoxal, 5 mL of 95% ethanol was added and the mixture was heated with constant stirring until the 2,2'-difluoro-diphenyl glyoxal, was completely dissolved. This was followed by the dropwise addition of 3.5 mL of aqueous (1N) potassium hydroxide. The reaction mixture was stirred and allowed to reflux well for 30 minutes. After completion of reaction, the mixture was cooled in an ice-water bath, potassium diphenyl glycolate was formed. This solution was cooled and poured into crushed ice containing 10mL of

1M HCl. The precipitate was filtered, washed with water and dried to afford 2,2'-diflouro diphenyl glycolic acid with yield of about 65%. The pH of the reaction mixture was maintained at 2 (Scheme 2.4).

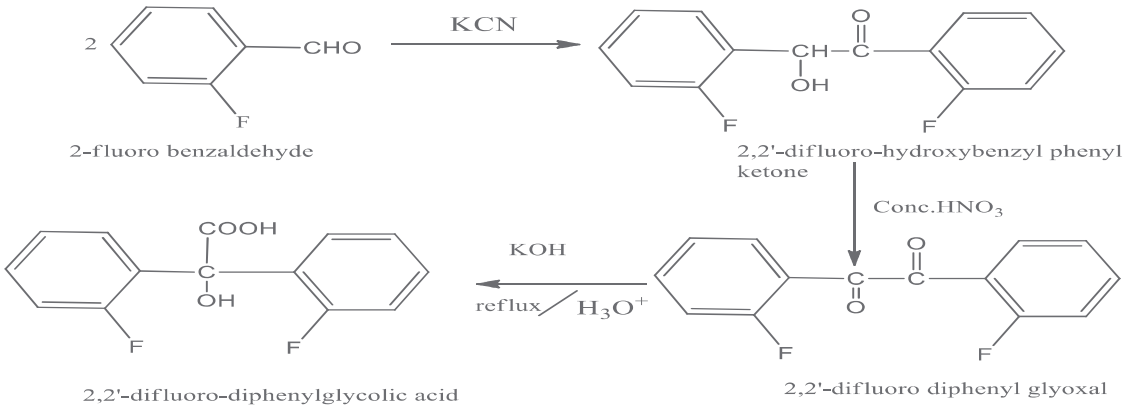

Scheme 1: Schematic representation of 2, 2'-DIFLUORO- DIPHENYL GLYCOLIC ACID

1.2 FTIR Spectral Analysis

The FTIR spectrum of the compound 2, 2'difluoro- diphenyl glycolic acid was recorded in the frequency region 4000 cm^{-1} - 450 cm^{-1}. 2, 2'difluoro- diphenyl glycolic acid molecules in the crystal lattice is greatly evident by the broadened envelope due to –OH stretch around 3437 cm^{-1}.

Table 1. Vibrational assignments of the 2,2'-diflouro diphenyl glycolic acid

FTIR (wave number) cm^{-1})	**Band assignments**
3437 cm^{-1}	-O-H stretching
1724 cm^{-1}	-C=O stretching
3066 cm^{-1}	Aliphatic C-H stretching
1567 cm^{-1}	Aromatic sym C=C stretching
1157cm^{-1}, 1065 cm^{-1}	C-O stretching

ISBN 978-816855382-8

The FTIR spectrum of the title compound shows the presence a strong intensity absorption at 1724cm^{-1} attributed to the C=O stretching of the carboxylic acid group. The bands around 3066cm^{-1} in FTIR are assigned to the C-H stretching. The C=C symmetric stretching vibrations of the aromatic ring observed by the band at 1567 cm^{-1}. The C-O stretching of the alcohol and carboxylic acid group are observed by the bands at 1157 and 1065 cm^{-1}.

1.3 Uv-Visible Spectral Analysis

The UV–visible spectrum was recorded between 200 and 900 nm, which gives the information about the aromatic portion of the molecule, because the absorption of UV and visible light involves promotion of the electron in the σ and π orbital from the ground state to higher states. The recorded UV–visible absorption spectrum for the synthesised compound is shown in Fig. 1. From the spectrum it is noted that the UV transparency cut-off around 266 nm and there is no significant absorption in the entire visible region of spectra. The transmission extends from 300 to 900 nm that makes it valuable for NLO applications involves blue/green light. Below 245 nm there is sudden increase in absorbance, due to the electronic transition in the aromatic ring and CO groups. Very good optical absorbance with the lower cut-off wavelength of 228 nm may be attributed to $\pi \rightarrow \pi^*$ and the broad absorption in the range of 245-289 nm corresponds to $n \rightarrow \pi^*$ transitions.

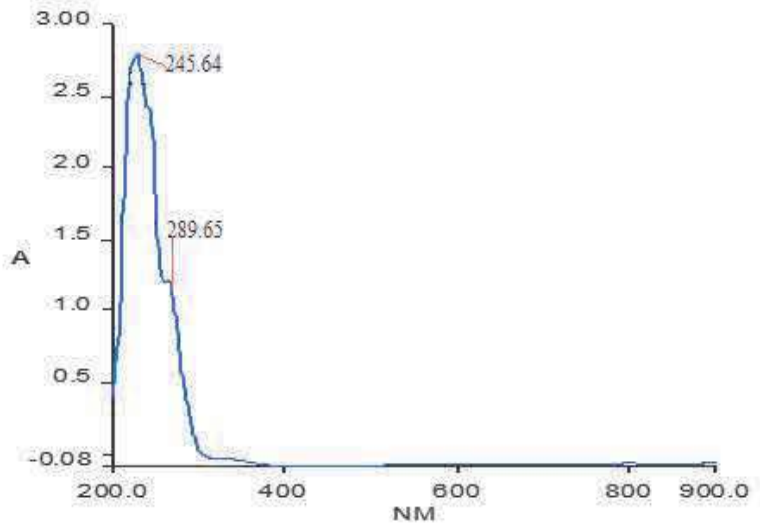

Figure 1: UV spectra of 2, 2'difluoro- 2, 2'difluoro- diphenyl glycolic acid in ethanol

2. Biological activity

2.1.Disc Diffusion Method

Antibacterial activity of the syntheised compound Diphenyl glycolic acid and 2, 2'-difluoro- diphenyl glycolic acid were carried by using disc diffusion method [98]. Petri plates were prepared with 20 ml of sterile MHA (Hi-media, Mumbai). The test culture (100µl of suspension containing 108 CFU/ml bacteria) were swabbed on the top of the solidified media and allowed to dry for 10 minutes. Three different concentrations of the compounds (25, 50 and 100 µg/disc) were loaded on a sterile disc and placed on the surface of the medium and left for 30 minutes at room temperature for compound diffusion [99]. Streptomycin (10 µg/disc) was used as a positive control [100]. These plates were incubated for 24 hrs at 37°C. Zone of inhibition was recorded in millimetres (mm).

ISBN 978-816855382-8

Micro Organisms Used

In vitro antimicrobial studies were carried out against different human pathogens. The three Gram-positive bacteria studied were Bacillus subtilis (ATCC 441), Staphylococcus aureus (ATCC 25923), Staphylococcus epidermidis (MTCC 3615) and the two Gram-negative bacteria studied were E.coli (ATCC 25922), Klebsiella pneumonia.

2.2 Results and Discussion of Experimental Study Antimicrobial Activity

The results revealed that the activity was considerably affected by various substitutions on the aromatic ring of Diphenyl glycolic acid. For antibacterial activity it was observed that introduction of electron withdrawing group on benzene ring of Diphenyl glycolic acid shows considerable increase in antibacterial potency of the compound.

Table 2. Anti-bacterial activity for different substituted Diphenyl glycolic acid using disc diffusion method

Name of the Pathogens	Antibacterial activity – Disc diffusion method (µg)						Streptomycin (S10)
	Zone of Inhibition (mm)						
	Difluoro- diphenyl glycolic acid			2,2-'difluoro-diphenyl glycolic acid			
	25	50	100	25	50	100	
Bacillus subtilis	-	-	-	-	-	-	9
Staphylococcus aeureus	-	5	-	-	-	11	20
Staphylococcus epidermitis	-	-	-	8	-	8	24
E.coli	-	-	8	-	-	10	20
Klebsiellapneumoniae	-	-	-	-	9	10	21

It was showed significant potency against Gram–positive Staphylococcus aeureusbacteria (MIC=11Mm). The same substitution showed maximum inhibition against Gram–negative bacteria like Klebsiellapneumoniae and E.coli. This is further

enhanced by increasing the concentration of the compound dosage for all pathogens (Table 2). The susceptibility of the microbes to the compound was compared with standard antibiotic streptomycin.

3. Docking Study

Docking studies for the synthesised compounds were performed using Glide module of Schrodinger, LLC, 2015. Primarily, by using Glide module (Grid based ligand docking with energetics), the important interactions based on the reference ligand and the protein of interest in the flexible mode docking were examined. The Glide module with three modes of docking, high-throughput virtual screening (HTVS), standard precision (SP), and extra precision (XP) mode were employed sequentially. The XP mode was used for exhaustive sampling and advanced scoring, resulting in even higher enrichment. Finally the shortlisted hit molecules were selected based on the visual inspection of amino acid interaction, docking score and the active site cavity.

Table. 3 Docking score and ligand interaction results for the synthesised compound

S.No.	Compound Name	Docking score (kcal/mol)	Ligand Interaction
1.	Diphenyl glycolic acid	-5.069	Trp64
2.	2, 2’-difluoro- diphenyl glycolic acid	-6.121	Tyr157

ISBN 978-816855382-8

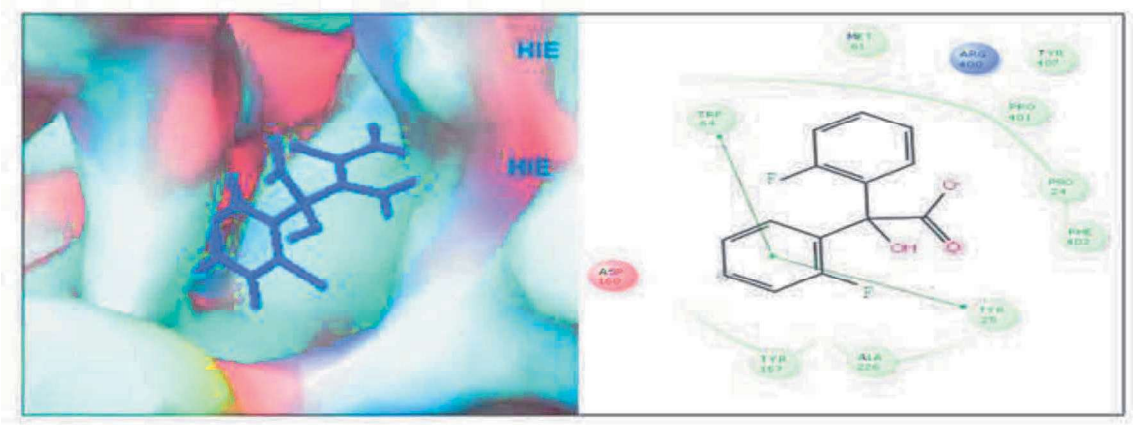

Figure 2: Binding analysis and ligand interaction diagram of diphenyl glycolic acid

The compound 2, 2'-difluoro- diphenyl glycolic acid was found to inhibit the bacteria at a distance of 6mm. This is quite lesser than the other molecules. This makes this molecule more effective binding and the docking score was found to be -6.121 kcal mol^{-1}. The binding analysis of this compound reveals that the compound well fitted into the active site pocket and the fluoro phenyl group was found to interact with non-polar amino acids Tyr25 and Trp64 which reveals that there are two stacking interactions making this compound more stable for further processing as better drug compound. The binding analysis and ligand interaction for the compound 2, 2'-difluoro-diphenyl glycolic acid was depicted in Fig. 1.

4. Conclusion

The synthesized compound diphenyl glycolic acid and its derivative mass and the presence of functional groups were analysed and confirmed by FTIR and UV analyses. To conclude, we have synthesized the diphenyl glycolic acid and its derivatives were docked into the protein which provides good binding energy and the interaction pattern. Compound 2,2'-difluoro- diphenyl glycolic acid

possessed good docking score with related to the reference ligand and it also possess the cancer cell toxic nature with the inhibition. Additional studies will be carried out with respect to the protein analysis and the binding affinity of the ligand through differential scanning fluorimetry experiments. A further study to acquire more information concerning pharmacological activity is in progress. More development of this group of compounds may lead to compounds with better pharmacological profile than standard drugs and serve as templates for the construction of better drugs to combat bacterial infection. After studying the docking poses and binding modes of the docked compounds, the necessity of hydrogen bond formation for enhancing the activity of this class of compounds can be highly advocated.

References

[1]. PR. Chandirana, D. Premnathb, SV. Kumara: Design, synthesis, molecular docking and antibacterial evaluation of novel n-(6, 11-dioxo-dihydro-5h-benzo [b] carbazol-2yl) benzamide derivatives as potent antibacterial agents. Int J Pharm Pharm Sci. Int J Pharm Pharm Sci, vol. 6, no. 6, pp. 244-249, 2014.

[2]. KS. Kumara, GA. Krishnamurthy, AS. Kumarn: Synthesis, characterization, in vitro antimicrobial, anthelmintic and docking studies of new 2-[(e)-{[4-(1h-1, 2, 4-triazol-1 ylmethyl) phenyl] imino} methyl] phenol, and their complexes with 3D metal ions. Int J Pharm Pharm Sci, vol. 8, no.9, pp.134-139, 2016.

[3]. A. Koul, E. Arnoult, N. Lounis, J. Guillemont, K. Andries: The challenge of new drug discovery for tuberculosis. Nature, vol. 469, pp. 483-490, 2011.

[4]. H. Gohlke, G. Klebe: Approaches to the description and prediction of the binding affinity of small-molecule ligands to macromolecular receptors. Angew Chem Int Ed Engl, vol. 41, no. 15, pp. 2644-2676, 2002.

[5]. A. Spannhoff, W. Sippl, M. Jung: Cancer treatment of the future: Inhibitors of histone Methyl transferases. Int. J. Biochem. Cell Biol, vol. 41, pp.4–1, 2009.

ISBN 978-816855382-8

[6]. T. Finkel, NJ. Holbrook: Oxidants, oxidative stress and the biology of ageing. Nature, vol. 408, pp. 239–247, 2000.

[7]. TS. Kang, HO. Jo, WK. Park, JP. Kim, Y. Konishi, JY. Kong, NS. Park, YS. Jung: Synthesis and antioxidant activities of 3, 5-dialkoxy-4-hydroxycinnamamides. Bioorg. Med.Chem. Lett. vol. 18, pp.1663–1667, 2008.

[8]. N. Noguchi: Novel insights into the molecular mechanisms of the anti-atherosclerotic properties of antioxidants: the alternatives to radical scavenging. Free Radical Biol. Med. Vol. 33, pp. 1480–1489 2002.

[9]. C. Foucault, P. Brouqui: FEMS Immunology and Medical Microbiology. Vol. 49, pp.173-184, 2007.

[10]. Neu, HC. The crisis in Antibiotic resistance. American Association for the advancement of Science. Vol. 257, pp. 1064-1080, 1992.

Chapter 9

Investigation of Lemon Seed oil biodiesel with Cerium Oxide Nanoparticle in CI Engine

Agaramudhalvan S[a]*, Shaisundaram V S[a]*

[a]Department of Mechanical Engineering, Vels Institute of Science, Technology & Advanced Studies, Chennai

** Corresponding Author: saiswastik23@gmail.com*

Abstract

Because of increasing automobiles, power plants and factories, increasing of this automobiles, power plants produce the more emissions like CO, HC and NOx. So that the world is searching for the alternative fuel, which will not create any harm to the environment and also it would be less in cost. Biodiesel is one of the main solutions to the global energy crisis. In this present work studied the performances and emission characteristics of Lemon Seed Oil Bio-diesel (GSO). Use of additives for better combustion characteristics to the biodiesel. The blends of Lemon Seed oil (GSO) with the additives Aluminum oxide are B10+20 PPM CeO_2, B20+20PPM CeO_2, B30+20 PPM CeO_2. This blends were analyzed and their performance and emissions characteristics compared with performance and emission characteristics of diesel. Tests were carried out over entire range of engine operation at varying conditions of load. The engine exhaust gas emissions are reduced with increase biodiesel concentration.

Keywords: Lemon Seed oil (LSO); Cerium oxide; Engine Performance characteristics, Exhaust emission characteristics.

ISBN 978-816855382-8

1. Introduction

In the context of fast depletion of fossil fuels and ever increasing diesel vehicle population, use of renewable fuels like vegetable oils has become pertinent steady with the estimation the International Energy Agency, by 2025 global energy utilization will increase by about 42%. Many research works are going on to substitute the diesel fuel with appropriate alternative fuel such as bio diesel. Bio diesel are best alternative for the diesel vehicle and it is easy to produce from the seeds and flowers. [1] has made an endeavor to discover the appropriateness of Trans esterified mahua oil as a fuel in C.I. motor. Trial work was done on 7B.H.P single chamber four stroke and vertical, water cooled Kirloskar diesel motor at evaluated speed of 1500rpm various mixes of trans esterified mahua oil with diesel were tried at 200bar infusion pressure. Slight increment in brake warm productivity and diminishing in explicit fuel utilization is seen on account of esterified mahua oil (all mixes particularly 75% mahua oil) contrasted with that of diesel. [2] Talked about the non-sustainable power sources are draining at higher way so there is more vitality request. Biodiesel is a trade for diesel fuel in packed start motors because of its noteworthy natural advantages. The utilization of biodiesel prompts decreases in PM, HC and CO discharges and the expansion in fuel utilization and the increment in NOx emanation on diesel motors with no change. The expansion of nano particles in biodiesel builds the warm proficiency and diminishes the NOx outflow. [3] assessed the impact of added substances (diethyl ether) and nano added substances (cerium oxide) in the mango seed oil methyl ester (MSME) biodiesel on motor execution, ignition and emanation attributes of four stroke direct infusion diesel motor. The brake thermal efficiency (BTHE) is improved with expansion of diethyl

ether and cerium oxide. The brake explicit fuel utilization (BSFC) and fumes gas temperatures (EGT) are diminished.

[4] Explored the impact of Alumina Metal Oxide (Al2O3) Nano Particles as added substance for Palm Stearin Methyl Ester Biodiesel (B 100) and their mixes as a substitute fuel in four stroke single chamber water cooled, direct infusion diesel motor. The NOX outflows were diminished by 9.70% for 50ppm alumina nano molecule mixed with palm stearin methyl ester contrasted with diesel. [5] discussed about the effect of mahua oil on diesel engines since diesel engines are major contributors of many air polluting exhaust gasses such as carbon monoxide, unburned hydrocarbons, oxides of nitrogen and other harmful compounds. [6] developed enthusiasm for biodiesel owing to the closeness in its properties in contrast with those of diesel energizes. There is a little improvement in results using the blends and the emissions are also low compared to the diesel.

[7] assessed the exhibition and emanation attributes of a single cylinder direct injection constant speed diesel engine with Soapnut oil. Soapnut oil, a nonedible straight vegetable oil was mixed with oil diesel in different extents to assess the presentation and discharge qualities of a single cylinder direct injection consistent speed diesel Engine. [8] talked about cleanser nut oil, cotton seed oil methyl ester and diesel were mixed in the extent of 10:15:75 by volume to shape a bio diesel mix of B25. It has been seen that the calorific worth is lower and consistency is higher for B25 when contrasted with diesel. [9] Pongamia as biodiesel were tested for their performance in diesel engines. The biodiesel for various proportions like 5%, 10%, 15% and 20% and the effect on diesel engine performance is studied. The effect of use of biodiesel on engine power, consumption of fuel and heat loss involved are collected and analyzed with that of conventional diesel.

ISBN 978-816855382-8

[10] talked about the objective of the current work is to audit the writing with respect to the basic parts of burning clamor radiation during transient activity of normally suctioned and turbocharged diesel engine.

2. Preparation of Biodiesel sample

The Nano particles bio diesel fuel is set up by blending the Cerium oxide nano particles in the Lemon seed oil with the guide of a ultrasonicator. The ultrasonicator procedure is the most appropriate technique to scatter the nano particles in base fuel (Lemon seed oil), as it encourages conceivable agglomerate nanoparticles back to nanometer go. Nano particles are for the most part having higher surface territory and henceforth surface vitality will be high and it will in general agglomerate to frame a smaller scale atom and begins to silt. So as to make nano molecule to be steady in a base liquid, it ought to be developed to surface adjustment. Consequently, the molecule sedimentation was controlled. So as to scatter the nano molecule to base liquid ultra-sonication system was followed. A known amount of (state 20 mg) added substance were gauged and poured in the biodiesel and ultrasonicated for 60 minutes. Then it forms a stable nano fluid.

3. Experimental Setup

A 5HP (5.2 kW) 4-Stroke direct injection research diesel engine was chosen to investigate the performance and combustion characteristics. The air flow rate into the engine was measured by mass flow sensor and the fuel consumption was measured by burette method. Loading was applied on the engine with the help of eddy current dynamometer. The experiment was carried at different loads. Various sensors were utilized during the experiment to collect, store

and analyze the data by computerized data acquisition system (IC engine soft). An exhaust gas analyzer (AIRREX HG-540, 4Gas analyzer) was employed to measure HC, CO, CO2 and NOX emissions. The performance, combustion and emission results obtained were tabulated. The engine setup is shown in fig 3.1

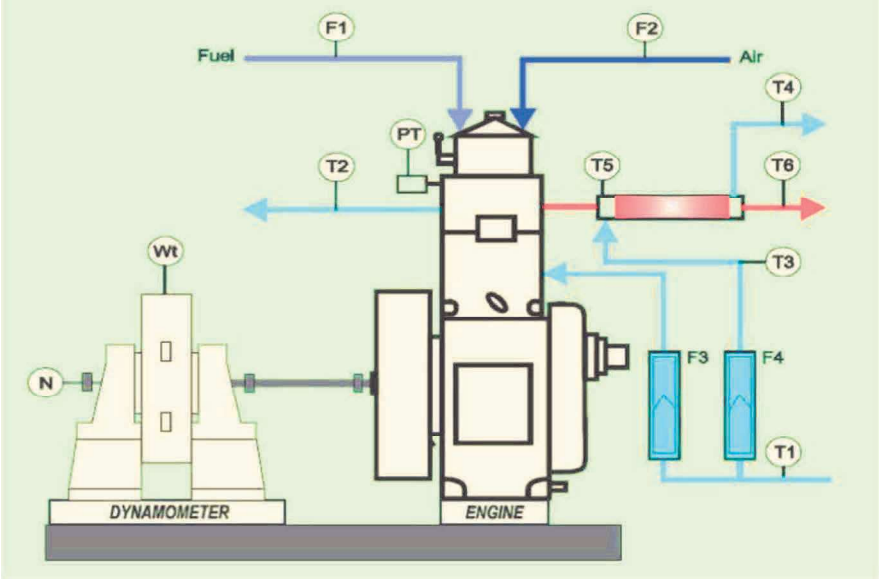

Figure 1: Experimental Setup

4. Results and Discussion

4.1 Brake Thermal Efficiency

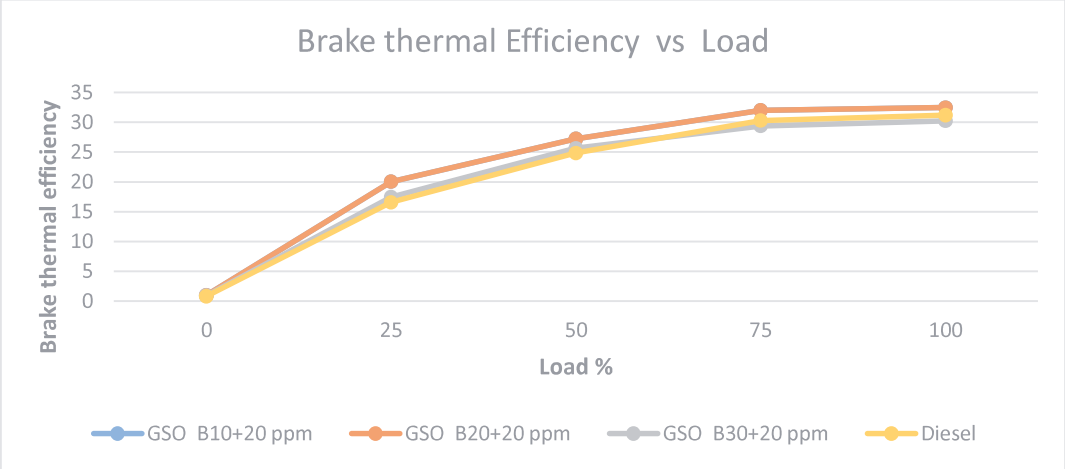

Figure 2: Brake thermal Efficiency Vs Load

ISBN 978-816855382-8

The brake thermal efficiency improved with improve in brake power. Fig.4.1 shows the variation of BTHE with BP for Lemon seed oil at various combinations nano additives comparing with diesel. B30 + 20 ppm aluminum oxide (24.5%) shows BTHE similar to that of neat diesel (27.80 %) at full load. The oxides of metal nano particles present in the biodiesel blend promote the complete combustion, while compared to the individual biodiesel blend.

4.2 Specific Fuel Consumption

The variation of SFC with BP of GSO modified biodiesel with different dosage level of Nano additives comparing with diesel. Corresponding to BP is shown in fig 4.2, SFC is decreasing while increasing the BP. At full load, SFC is higher for B30 (0.24 kg/kWh) adding with Nano particles but it attains 8% lower value for diesel (0.28 kg/kWh). CONP, oxidize the carbon deposits in the engine cylinder to reduced fuel consumption.

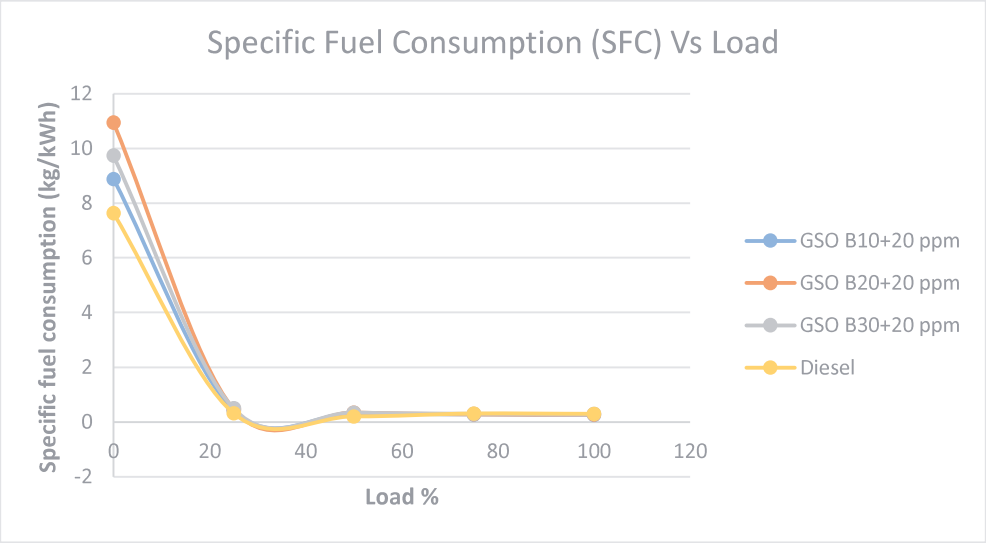

Figure 3: Specific Fuel Consumption Vs Load

4.3 Hydrocarbon (HC)

The variation of HC with Load for B10, B20, B30 and modified blends is shown in Fig 4.3. The HC increases with Load for all the blends. However, HC emissions are found to be considerably reduced with the addition high ppm of nano particles. Fundamentally, the oxygen content of fuel is the main reason for hydro carbon emissions reduction.

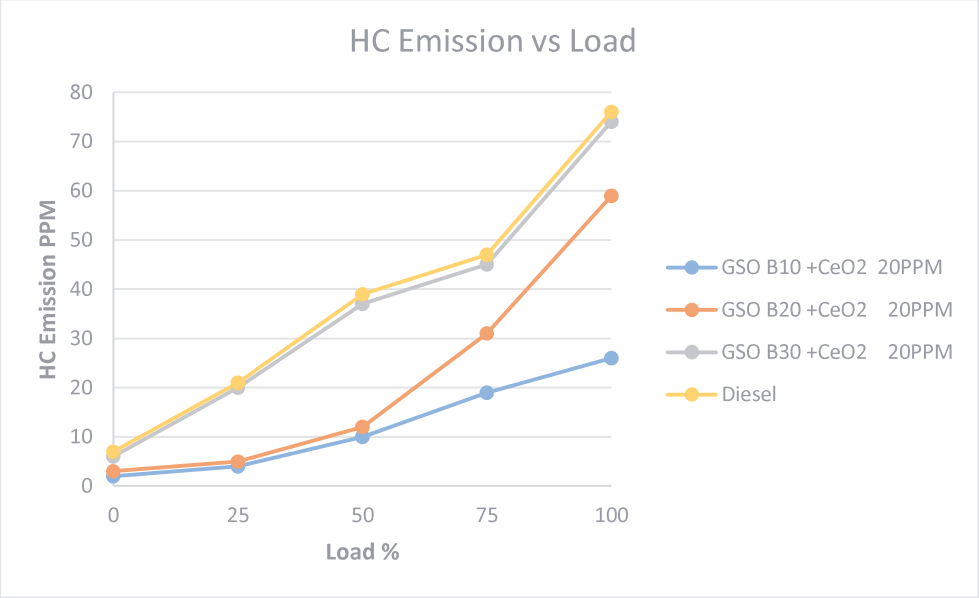

Figure 4: Hydrocarbon Vs Load

4.4 Carbon monoxide

The influence of additives to biodiesel on carbon monoxide emissions is shown in fig 4.4 CO emissions are increasing while increasing the Load for all the blends. Hence CO emissions shows lower values for B10, B20, and B30 blend adding CeO_2 additives. This may be combustion improvement due to adding CeO_2. Because of incomplete combustion causes CO emissions.

ISBN 978-816855382-8

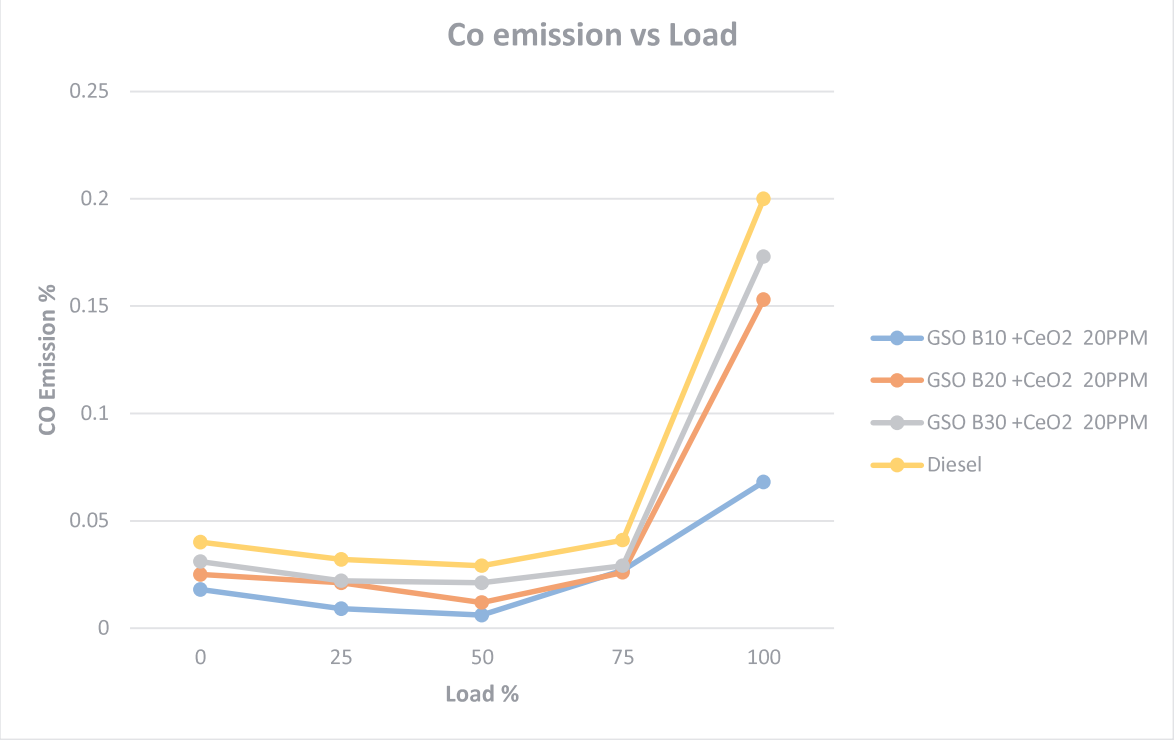

Figure 5: Carbon monoxide Vs Load

4.5 Nitrogen Oxides (NOx)

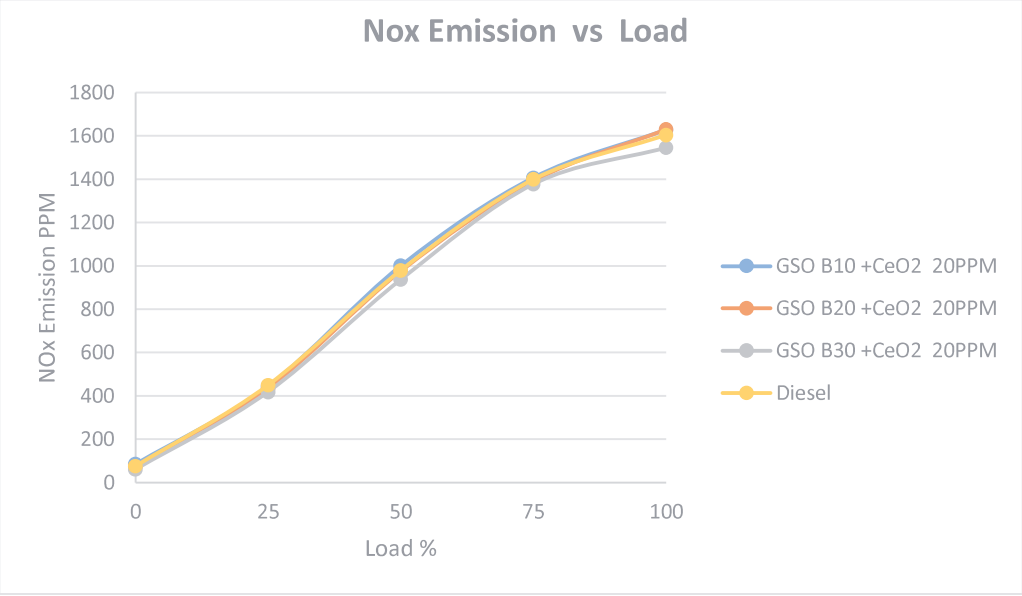

Figure 6: Nitrogen oxides Vs Load

The variation of nitrogen oxides with load for different blends of biodiesel is illustrated in fig 4.5. Nitrogen oxides are mainly formed due to high temperatures. NO_X is increasing with Load however diesel values are lower than all blends having nano particles

5. Conclusion

The experiment was conducted to investigate the effects of Cerium oxide (CeO_2) Nano particle as an additive for Lemon seed oil on Performance, combustion and emission characteristics of CI engine, based on the experiments the following conclusions are drawn:

- The brake thermal efficiency was almost same for diesel and Lemon seed oil blended with Aluminum oxide (20 ppm)
- By using Lemon seed oil blended with Cerium oxide (20 ppm) the carbon monoxide (Co) emission were decreased compared to diesel.
- Lemon seed oil blended with Cerium oxide (20 ppm) has higher NOx emissions
- NOx emissions of Lemon seed oil methyl ester blended with Cerium oxide (150 ppm) has lesser Nox emission compared with other blends
- On the whole it is concluded that 150 ppm of Cerium oxide can be used as additive which showed reduction in emissions as well as compatible performance and combustion characteristics with Lemon seed oil biodiesel

References

[1] Abdalla, S., Al-Wafi, R., & Pizzi, A. (2017). Stability and combustion of metal nano-particles and their additive impact with diesel and biodiesel on engine efficiency: A comprehensive study. *Journal of Renewable and Sustainable Energy*, *9*(2), 022701.

ISBN 978-816855382-8

[2] Tajudeen, S., & Velraj, R. (2014). Nanoadditives: enhancement of combustion and performance characteristics of a CI diesel engine. International Journal of Applied Environmental Sciences, 9(4), 1727-1741.

[3] Shaisundaram, V. S., Chandrasekaran, M., Mohan Raj, S., & Muraliraja, R. (2020). Investigation on the effect of thermal barrier coating at different dosing levels of cerium oxide nanoparticle fuel on diesel in a CI engine. International Journal of Ambient Energy, 41(1), 98-104.

[4]. Shaisundaram, V. S., Chandrasekaran, M., Shanmugam, M., Padmanabhan, S., Muraliraja, R., & Karikalan, L. (2019). Investigation of Momordica charantia seed biodiesel with cerium oxide nanoparticle on CI engine. International Journal of Ambient Energy, 1-5.

[5]. Shaisundaram, V. S., Chandrasekaran, M., Mohan Raj, S., Muraliraja, R., & Vinodkumar, T. (2019). Control of carbon dioxide emission in automobile vehicles using CO2 scrubber. International Journal of Ambient Energy, 40(7), 699-703.

[6]. Shaisundaram, V. S., Karikalan, L., & Chandrasekaran, M. (2019). Experimental Investigation on the Effect of Cerium Oxide Nanoparticle Fuel Additives on Pumpkin Seed Oil in CI Engine. International Journal of Vehicle Structures & Systems (IJVSS), 11(3),

[7]. Muraliraja, R., Sudagar, J., Elansezhian, R., Raviprakash, A. V., Dhinakaran, R., Shaisundaram, V. S., & Chandrasekaran, M. (2019). Estimation of Zwitterionic surfactant response in electroless composite coating and properties of Ni–P–CuO (Nano) coating. Arabian Journal for Science and Engineering, 44(2), 821-828.

[8]. Muraliraja, R., & Elansezhian, R. (2015). Influence of nickel recovery efficiency on crystallinity and microhardness of electroless Ni–P coatings and optimisation using Taguchi technique. Transactions of the IMF, 93(3), 126-132.

[9]. Muraliraja, R., Sendilkumar, D., & Elansezhian, D. R. (2015). Prediction and Supplementation of Reducing Agent to Improve the Coating Efficiency and Wear Behavior of Electroless Ni-P Plating. Int J Electrochem Sci, 10, 5536-47.

[10] S.Baskar, V. Vijayan, S. Saravanan, A.V. Balan & A. Godwin Antony, “Effect of Al2O3, Aluminium Alloy and Fly Ash for Making Engine Component”, International Journal of Mechanical Engineering and Technology (IJMET), Volume 9, Issue 12, December 2018, pp. 91-96.

Chapter 10

Experimental investigation on the effect of Cerium Oxide nanoparticle fuel additives on sapota seed oil in CI engine

Agaramudhalvan S[a]*, Shaisundaram V S[a]*

[a]Department of Mechanical Engineering, Vels Institute of Science, Technology & Advanced Studies, Chennai

** Corresponding Author: saiswastik23@gmail.com*

Abstract

Major portion of today's energy demand in the world is being satisfied with fossil fuels. On the record of confronting the up and coming energy crisis, bio oils have come up as a promising source of fuel for IC Engines. As India is an agricultural country, there is a wide extension for the generation of vegetable oils (both edible and non-edible) from various plant assets. This is the reason that colossal research work is going ahead to utilize bio oil as fuel. But there is a serious perception that the performance and efficiency of bio oils is found to be less than that of mineral diesel. This research work is to prove that with necessary modifications in Compression ignition engine the efficiency can be improved and it can be made equivalent or still better than mineral diesel. Sapota Seed Oil is one among them that is available abundantly in India and all over the world. An experimental investigation was made to evaluate the performance and emission characteristics of a diesel engine using different blends of Sapota seed oil with cerium oxide Nano particle additive is added in diesel. Sapota seed Oil was blended with diesel in proportions of 10%, 20%, and 30% by volume, performance and Emission parameters was

ISBN 978-816855382-8

studied under different loading conditions in compression ignition engine.

Keywords - compression ignition engine, Sapota seed Oil, cerium oxide additives, performance, emission.

1. Introduction

Due to the oil embargo and subsequent War, it was very crucial problem of best utilization of energy for both developed and developing countries. Then, it was the first time that the crude petroleum importing nations stroked the shock when the oil exporting countries bargained higher prices. This crucial energy crisis forced all the countries to look for unconventional sources of energy (renewable energy) and proficient utilization of energy. Then the focus of the country planners has been changed to more efficiency, extra productivity and least production cost. This resulted in an abrupt, long term and multi-aspect solution to the problems emerging from short supplies and increased energy demands throughout the world. Nowadays world is facing the twin problems of fast exhaustion of fossil fuels and environmental degradation. Hence, there is an urgent need to reduce dependence on petroleum derived fuels for better economy and environment. Adaptation of bio-origin unconventional fuels can address both these issues. These fuels are basically non-petroleum and result in energy security and environmental benefits.

Hossain. A.K et al [1] tested a multi-cylinder water cooled CI engine with karanja oil. The engine cooling water circuit and fuel supply systems were modified such that hot coolant preheated the biodiesel prior to injection. Compared to fossil diesel, the BSFC was 3% higher for the plant oils and the brake thermal efficiency was almost similar which resulted in higher CO2 and NOx emissions.

AshfaqueAhmed.S et al [2] analyzed by blending the lemongrass oil with diesel with different proportions and testing the performance of blended diesel. The tests were carried out for raw lemongrass oil, 20% lemongrass oil, 40% lemongrass oil, 80% with diesel. The performance was studied and it is concluded that, the blending of 20%, 40%, 60%, 80% and 100% at room temperature gives better fuel consumption and also improves emission norms.

SenthilKumar.S et al [3] investigated the performance and emission characteristics of a diesel engine fueled with diesel and blends of rubber seed oil based bio-diesel compared to that of diesel. Engine performance with biodiesel does not differ greatly from that of diesel fuel. The experimental results proved that the use of rubber seed oil based biodiesel is viable alternative to diesel. Ibrahim Khalil Adam et al [4] in this study rubber seed/palm oil mixture at equal blend ratio was used to produce biodiesel. Parametric effect on transesterification were studied using response surface methodology.

Tiwari et al [5] discussed in developing country, India is in need of potential bio-diesels that are derived from non-edible vegetable oils to minimize the dependency on petro diesel, thus reducing the foreign expenditure on crude oil import, as well as to meet the environmental concerns. For the reason, in the present work, feasibility of soap nut bio-diesel as a potential alternate fuel for diesel engine, as well as engine performance parameters of a single cylinder four stroke diesel engine using petro-diesel and lean soap nut biodiesel blends with petro-diesel as engine fuels, were experimentally investigated. The experimental investigation showed soap nut bio-diesel to be a potential alternate fuel for diesel engine. Moreover, lean soap nut bio-diesel blends exhibited satisfactory engine performance over the entire load range with performance of 10% blend of soap nut bio-

ISBN 978-816855382-8

diesel with petro-diesel i.e. B10 being marginally better than the petro-diesel as well as other blends.

From the literature study, it is observed that many researchers have used variety of biodiesel along with the conventional diesel fuel in the analysis of combustion, performance and emission of a wide range of diesel engines with little or without modification. In this project work, bio-fuel blends from Sapota seed oil is explored in its performance and emission characteristics in single cylinder diesel engine to observe a substitute fuel by comparing the blended fuel results with base pure diesel.To study the performance and emissions characteristics of Sapota seed oil as biodiesel on single cylinder VCR diesel engine.To study the performance and emissions characteristics of various blends (B10, B20, B30) of Sapota seed oil as biodiesel with cerium oxide additive. To find an alternative by comparing the results of Sapota seed oil biodiesel blends with base fuel performance and emissions characteristics.

1.1 Sapota Seed Oil as Bio-Diesel

Transesterification of natural glycerides with methanol to methyl-esters is a technically important reaction that has been used extensively in the soap and detergent manufacturing industry worldwide for many years. Almost all biodiesel is produced in a similar chemical process using base catalyzed transesterification as it is the most economical process, requiring only low temperatures and pressures while producing a 98% conversion yield. The transesterification process is the reaction of a triglyceride (fat/oil) with an alcohol to form esters and glycerol. A triglyceride has a glycerine molecule as its base with three long chain fatty acids attached. The characteristics of the fat are determined by the nature

of the fatty acids attached to the glycerine. The nature of the fatty acids can, in turn, affect the characteristics of the biodiesel.

During the esterification process, the triglyceride is reacted with alcohol in the presence of a catalyst, usually a strong alkaline like sodium hydroxide. The alcohol reacts with the fatty acids to form the mono-alkyl ester, or biodiesel, and crude glycerol. In most production, methanol or ethanol is the alcohol used (methanol produces methyl esters, ethanol produces ethyl esters) and is base catalyzed by either potassium or sodium hydroxide. Potassium hydroxide has been found more suitable for the ethyl ester biodiesel production, but either base can be used for methyl ester production.

The equation below shows the chemical process for methyl ester biodiesel. The reaction between the fat or oil and the alcohol is a reversible reaction, so the alcohol must be added in excess to drive the reaction towards the right and ensure complete conversion.

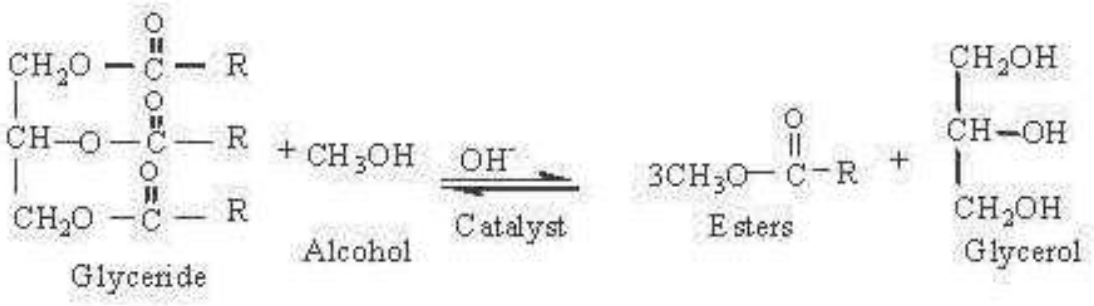

The products of the reaction are the biodiesel itself and glycerol. A successful transesterification reaction is signified by the separation of the methyl ester (biodiesel) and glycerol layers after the reaction time. The heavier co-product, glycerol, settles out and may be sold as is or purified for use in other industries, e.g. pharmaceutical, cosmetics, and detergents.

ISBN 978-816855382-8

After the transesterification reaction and the separation of the crude heavy glycerin phase, the producer is left with a crude light biodiesel phase. This crude biodiesel requires some purification prior to use. Biodiesel has a viscosity similar to petroleum diesel and can be used as an additive in formulations of diesel to increase the lubricity.

Biodiesel can be used in pure form (B100) or may be blended with petroleum diesel at any concentration in most modern diesel engines.Biodiesel is a better solvent than petroleum diesel and has been known to break down deposits of residue in the fuel lines of vehicles that have previously been run on petroleum diesel. Fuel filters may become clogged with particulates if a quick transition to pure biodiesel is made, as biodiesel "cleans" the engine in the process. It is, therefore, recommended to change the fuel filter within 600-800 miles after first switching to a biodiesel blend.

2. Preparation of Sapota Seed Biodiesel

Figure 1: Sapota Seed Oil

After transesterification the oil which we get has still higher viscosity to reduce it the next step is blending. By blending the oil can be handled easily it is the main purpose to reduce the volatility. In order

to evaluate the biodiesel in the CI engine, various blends of Soap nut seed oil and the conventional diesel has been prepared by mixing with the different amounts of diesel and biodiesel. In this study the blends of B10, B20 and B30 were prepared for testing.

Biodiesel is available in a number of different blends. It can be used as a fuel on its own (B100), or blended with diesel into B5, B10 etc.

Table 1. Properties of Sapota seed oil

Sl.No	Property	Value
1	Density	0.930g/cc
2	Kinematics viscosity@40 ℃	9.99cSt
3	Flash point by PMCC method	238 ℃
4	Fire point by PMCC method	254 ℃
5	Calorific value	6978.953 cal/g

Addition of cerium oxide to diesel cause significant reduction in number weighted size distributions and light-off temperature and the oxidation rate was increased significantly. Cerium oxide being a rare earth metal with dual valance state existence has exceptional catalytic activity due to its oxygen buffering capability, especially in the Nano sized form. Hence when used as an additive in the diesel fuel it leads to simultaneous reduction and oxidation of nitrogen dioxide and hydrocarbon emissions, respectively, from diesel engine.

Table 2. Properties of Cerium Oxide

ISBN 978-816855382-8

Molecular formula	CeO_2
Molar mass	172.115 g/mol
Appearance	White or pale yellow solid, Slightly Hygroscopy
Density	7.215 g/cm^3
Melting point	2,400 °C (4,350 °F; 2,670 K)
Boiling point	3,500 °C (6,330 °F; 3,770 K)
Solubility in water	Insoluble
Crystal structure	Cubic (fluorite)

The blending of Sapota seed biodiesel with cerium oxide is mainly done by sonication process. Hielscher offers ultrasonic mixing reactors for the production of biodiesel at any scale. The ultrasonic mixing improves mass transfer and reaction kinetics leading to faster transesterification and higher yield. It saves excess methanol and catalyst.

3. Experimental Set Up

A Single cylinder, constant speed, Direct Injection engine was used to evaluate the engine performance and emission characteristics of plastic oil. The diesel runs under different load conditions at a constant speed of 1800 rpm with the different plastic oil proportions. The diesel engine was directly attached with an eddy current dynamometer for varying the loads from no load (0%) to full load (100%). Based on the engine power, the engine load is varied from no load condition of 0%, 25%, 50%, 75% and full load condition of 100%.

The engine loads are varied manually with help of an eddy current dynamometer. Air flow rate was measured with an air drum fitted with a calibrated orifice and the fuel flow was measured using volumetric (calibrated burette) method. For fuel flow measurement, two fuel tanks were used; one is filled with pure diesel while esterified plastic oil is filled in another fuel tank. An AVL smoke meter was attached for measuring the smoke opacity and exhaust gas temperatures. The test rig was installed with AVL Indi micro software to obtain various readings and results during operation. A five gas analyzer was used to measure the emission characteristics such as UHC, CO, NO_x, CO_2 and O_2 values from the exhaust gas. The performance and emission tests were conducted at the compression ratio of 17.5 and with rated power.

The test was carried out for different proportions of waste plastic oil blended with the pure diesel fuel. The performance analysis of the engine at different rated power was evaluated in terms of Brake Specific Fuel Consumption (BSFC), Brake Thermal Efficiency (BTE) and emissions characteristics such as UHC, CO, CO2 and NO_x. The photographic view of the experimental set up used in this study.

4. Results and Discussion

5.1 Performance

5.1.1 Brake Thermal Efficiency

The performance of the brake thermal efficiency for different loads with blended fuel at different ratios of diesel, Sapota seed oil.The higher viscosity of the blended fuel reduced the brake thermal efficiency and the blended fuel was similar to that of the diesel performance. It is observed that, at maximum load condition and it was only 2% variation from that of the pure diesel performance.

ISBN 978-816855382-8

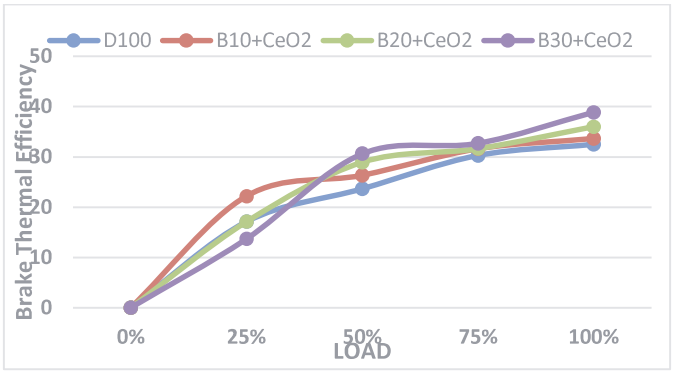

Figure 2: Load Vs BTE

5.1.2 Specific Fuel Consumption

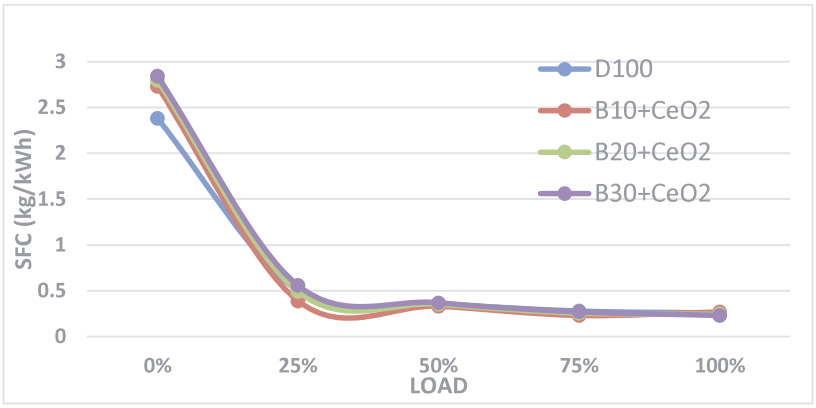

Figure 3: Load Vs SFC

The Specific fuel oil consumption of blended oil is slightly higher than diesel oilit is derived that the diesel has a lower Specific fuel oil consumption because of high calorific value, with blended fuel B10 the equivalent SFC was very closer but higher than that for the pure diesel fuel. This was observed due to the slightly lower calorific value and higher viscosity of the biofuel.

5.2 Emission Characteristics

5.2.1 Carbon MonoOxide

The emission characteristics was carried out for different blends of biofuels with the pure diesel fuel. The emissions characteristics of CO analyzed with cerium oxide additives. The Carbon Monoxide emissions from blended fuel are a bit more than the normal diesel fuel at all loads. Diesel engines produce little amount of CO when compared to NO_x and particulate emission as the engine was not loaded.

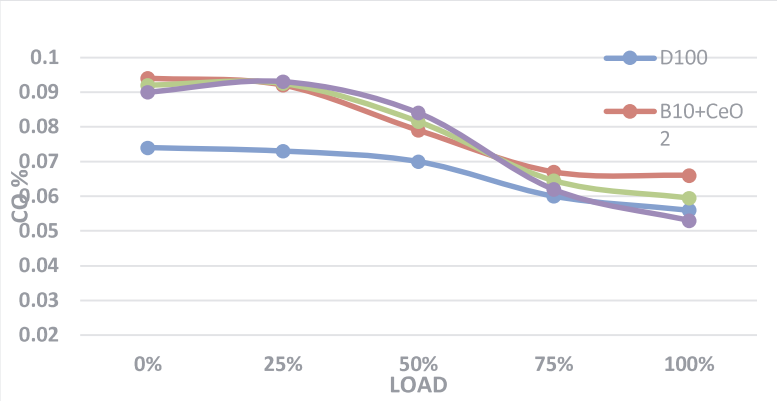

Figure 4: Load Vs CO

5.2.2 Carbon Dioxide

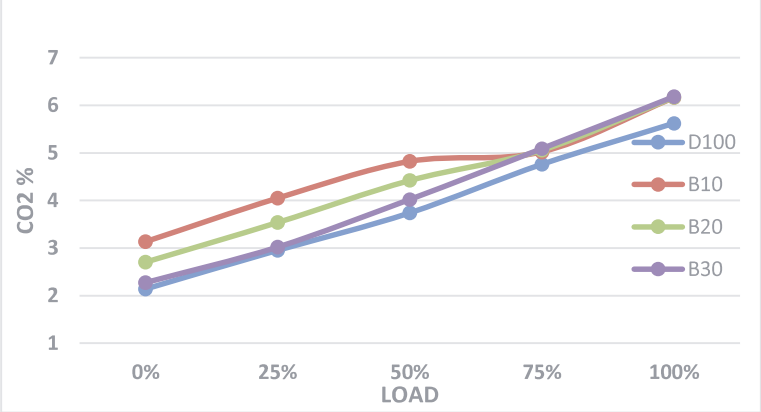

Figure 5: Load Vs CO

ISBN 978-816855382-8

The emission test was carried out for different proportions of biofuel blended with the pure diesel fuel. The emissions characteristics ofCO_2 analyzed with and without nano additives. From the readings, it is inferred that emission of Caron dioxide is slightly higher than pure diesel. The CO emission can be reduced by providing surplus oxygen in to the combustion chamber. There by converting CO into CO_2 this is possible by complete combustion.

5.2.3. Hydro Carbon

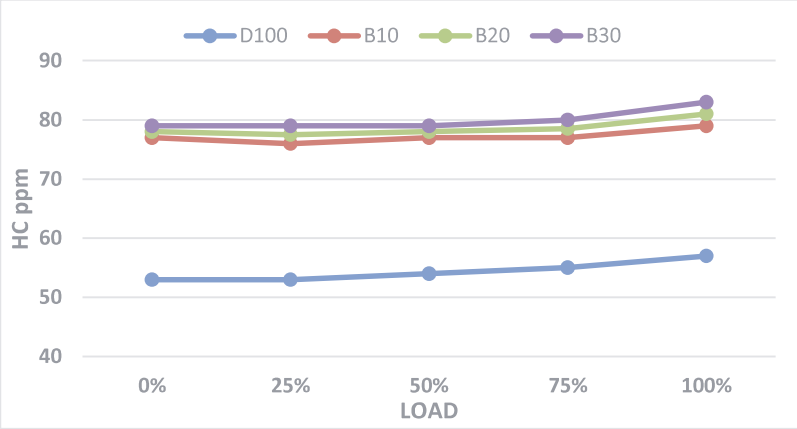

Figure 6: Load Vs HC

The test was carried out for different proportions of biofuel blended with the pure diesel fuel. The emissions characteristics of HC analyzed with and without nano additives. At different load conditions, the unburned hydrocarbon emission was lower for the diesel fuel with respect to the blends of Sapota seed oil as shown in Fig. 5.2.3. This is because of the higher calorific value of diesel and due to which less amount of fuel was injected when compared to bio fuel. Because of oxygen enrich environment, combustion is complete. Hence lower unburned hydrocarbon emission was observed with diesel fuel.

5.2.4. Nitrogen Oxides

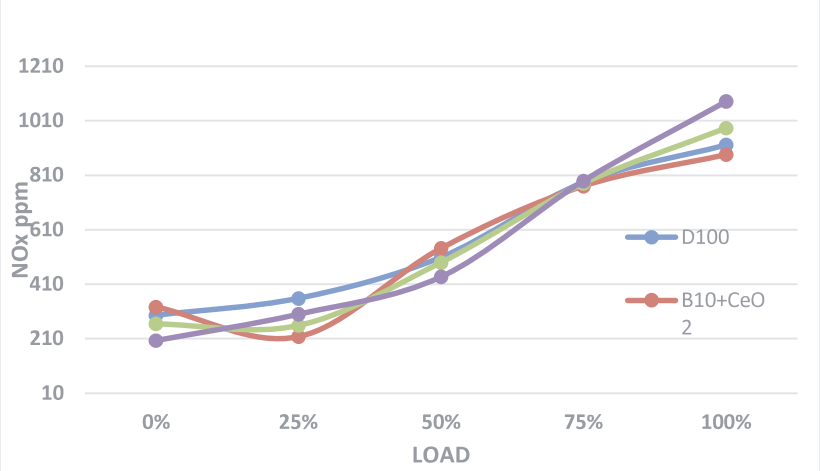

Figure 7: Load Vs NOx

The study of nitrogen oxide emission from diesel, Sapota seed oil blends are slightly lower than the pure diesel fuel performance at maximum loads and it was shown in Fig. 5.2.4. Because of more air action, much elevated than stoichiometric values, diesel engines produce more NOx at part load conditions and at higher loads. Diesel has higher calorific value than that of Sapota seed oil, so a lesser amount of diesel was injected into the combustion chamber.

6. Conclusion

In this work, bio fuel from Sapota seed blends has been attempted as an alternative fuel. The experiments were conducted without any modification on the engine. CI engine performance tests were conducted with three blend ratios of Sapota seed oil with diesel. Based on the engine performance and emission characteristic test of the Sapota seed oil an admirable substitute fuel which gives better performance and similar emission characteristics results compared with base pure diesel.

ISBN 978-816855382-8

References

[1] Hossain, A. K., & Davies, P. A. (2012). Performance, emission and combustion characteristics of an indirect injection (IDI) multi-cylinder compression ignition (CI) engine operating on neat jatropha and karanj oils preheated by jacket water. *Biomass and bioenergy*, *46*, 332-342.

[2] Ashfaque Ahmed., Prabhakar. S., and Binu. K. Soloman and Soloman. K. (2013) "Performance Test for Lemon Grass Oil in Twin Cylinder Diesel Engine", ARPN Journal of Engineering and Applied Sciences, Vol. 8, No .6, pp.435-437.

[3] Senthil Kumar. S., and Purushothaman. K. (2012), "High FFA Rubber Seed Oil as an Alternative Fuel for Diesel Engine – An Overview" International Journal of Engineering and Science ISBN: 2319-6483, ISSN: 2278-4721, Vol. 1, Issue 10, pp.16-24.

[4] Ibrahim Khalil Adam, A. Rashid A. Aziz, and Suzana Yusuf (2016), "Response surface methodology optimization of palm Rubber seed combined oil based biodiesel and idi diesel Engine performance and emission", ARPN Journal of Engineering and Applied Sciences, Vol. 11, no. 24, pp 1819-6608.

[5] Tiwari A C (2015)," Effect of using blends of soapnut bio-diesel with petro-diesel as engine fuels on performance parameter of a single cylinder four stroke diesel engine" Volume 6, Issue 7, July 2015, pp. 28-38.

Smart Materials, Chemical Systems, and Digital Technologies

April 2026

Dr. R. MURALIRAJA is an Associate Professor and Associate Dean (International Affairs) with extensive academic and research experience in mechanical engineering. He holds a Ph.D. in surface coatings from Pondicherry Engineering College and has completed postdoctoral research in composite materials at Sultan Qaboos University, Oman. His research focuses on electroless coatings, metal matrix composites, and advanced manufacturing processes. He has published numerous SCI and Scopus-indexed papers and authored books and book chapters with reputed publishers such as CRC Press and Springer. Dr. Muraliraja has also led funded research projects and actively contributes to international collaborations, academic development, and engineering innovation.

Mrs. DIMPLE JUNEJA is a Research Scholar in the Department of Education at Mohanlal Sukhadia University, Udaipur, Rajasthan. She holds multiple qualifications, including M.Phil. in Commerce, M.Com., M.Ed., MBA (Finance & HR), M.A. in Economics, and a Certificate in Guidance. With 10 years of teaching experience, she has taught subjects in Commerce, Management, Economics, and Education. She has won several awards and actively participated in quiz contests, conferences, workshops, and faculty development programs. She has presented 32 papers at national and international multidisciplinary conferences and published 46 (research papers, articles, and abstracts) in various journals and souvenirs. She has also served as the editor of 36 books and 45 souvenirs. Dimple is a lifetime member of several professional organizations.

Dr. A. R. SIVARAM, M.E., Ph.D., is an Assistant Professor in the Department of Naval Architecture and Offshore Engineering at the Academy of Maritime Education and Training (AMET), Chennai, and serves as Associate Dean – Academics. With over 11.5 years of teaching and research experience, his expertise includes heat transfer, fuels, refrigeration and air-conditioning, and materials engineering. He has published 39 journal papers and 19 conference papers. He received the Best Oral Presentation Award at Anna University and First Prize at Urjavaran-2022 by ISHRAE and IGCAR. He secured ISHRAE SRPG funding for student projects and co-coordinated an AICTE ATAL FDP on Carbon Neutrality with ₹6 lakh funding.

Dr. S. GNANAM is an Assistant Professor in the Department of Physics at Vels Institute of Science, Technology & Advanced Studies (VISTAS), Chennai. He has over 12 years of teaching and 15 years of research experience. He completed his UG and PG with first-class distinction from the University of Madras and earned his Ph.D. from Presidency College, Chennai. He has published 72 research papers in international journals and presented 62 papers at conferences. His research focuses on nanoscience, crystal growth, and thin films. He has received multiple best paper awards and serves as a reviewer and guest editor for reputed scientific journals.

SCIENTIFIC RESEARCH REPORTS

(A Book Publisher, approved by Govt. of India)

I Floor, S S Nagar, Chennai - 600 087,
Tamil Nadu, India.
editors@srrbooks.in, contact@srrbooks.in
www.srrbooks.in

ISBN 978-81685538-2-8